

Copyright  
by  
Camila R. Fontes-Garfias  
2020

**The Dissertation Committee for Camila R. Fontes-Garfias Certifies that this  
is the approved version of the following dissertation:**

**Functional analysis of glycosylation of Zika virus envelope and NS1  
proteins**

**Committee:**

---

Pei-Yong Shi, PhD, Supervisor

---

Kyung Choi, PhD, Chair

---

Eric Wagner, PhD

---

Alan Barrett, PhD

---

Shelton Bradrick, PhD

---

Tian Wang, PhD

**Functional analysis of glycosylation of Zika virus envelope and NS1  
proteins**

**by**

**Camila R. Fontes-Garfias, B.S.**

**Dissertation**

Presented to the Faculty of the Graduate School of  
The University of Texas Medical Branch  
in Partial Fulfillment  
of the Requirements  
for the Degree of

**Doctor of Philosophy**

**The University of Texas Medical Branch**

**December 2020**

### **Dedication**

I dedicate this work to my baby girl, Andrea Camille Garfias. Andrea, mi vida entera eres tú, tú has sido mi motivación para lograrlo todo. Antes de estar en mi vientre, estuviste en mi corazón por muchos años siendo mi motor, mi fuerza, mi todo. En los días más oscuros, cuando el rendirse era muy atractivo, solo el pensar que un día tendría un bebé me daba las fuerzas para seguir adelante. Todo lo que he hecho ha sido pensando en ti. Hoy, escribo la culminación de demasiados años de estudio contigo en mi vientre y eternamente en mi alma. Espero que un día tú llegues aún más lejos que yo; le pido a Dios que me de sabiduría para guiarte y me permita verte siendo mujer sumamente exitosa. Andrea el mundo es tuyo pero nunca olvides que la verdadera clave de el éxito es el estudio, and most importantly, there is no substitution for hard work and discipline. I hope I can inspire you to pursue your dreams de la misma forma que tu has sido siempre mi inspiración.



## **Acknowledgements**

First, I want to acknowledge Dr. Shi for allowing me to join his lab, for believing in me, for sharing his enthusiasm, knowledge, and passion for science.

Dr. Shan, I would not be where I am without you. Thank you for being patient, supportive, and a fantastic mentor and friend. Thank you, Chao!

I want to acknowledge all the Shi lab members, past and present: Dr. Xuping Xie, Dr. Jing Zou, Dr. Hongjie Xia, Dr. Coleman Baker, Dr. Yang Liu, Dr. Yujiao Yang, Xianwen Zhang, Dr. Daniele Medeiros, Dr. Bruno Diniz Nunes, Jannyce Guedes da Costa Nunes, Antonio Muruato, Zengguo Cao, Dr. Dieudonné Buh Kum; for the fundamental support to this work and for making the difficult days in the lab enjoyable.

I am grateful to my committee members, Eric Wagner, Tian Wang, Alan Barrett, Kay Choi, and Shelton Bradrick, for the critical guidance leading me to complete my dissertation.

Thanks again to my parents, husband, brother, family, and friends for all their support during the last five years.

## **Functional studies of ZIKV replication and pathogenesis**

Publication No. \_\_\_\_\_

Camila R. Fontes-Garfias, PhD

The University of Texas Medical Branch, 2020

Supervisor: Pei-Yong Shi

Zika virus (ZIKV) infection causes devastating congenital abnormalities and Guillain-Barré syndrome. ZIKV has two important glycoproteins, both the envelope (E) protein, and nonstructural protein 1 (NS1). The ZIKV envelope (E) protein is responsible for viral entry and represents a major determinant for viral pathogenesis. NS1 forms a homodimer necessary for viral replication and it is also secreted as a hexamer and is involved in immune system evasion and pathogenesis. Like other flaviviruses, the ZIKV E protein is glycosylated at amino acid N154 and the NS1 is glycosylated at amino acids N130 and N207. To study the function of ZIKV protein glycosylation, recombinant ZIKV viruses were generated that lack the glycosylation sites, and the mutant viruses were analyzed in mammalian and mosquito hosts. In mouse models, the mutants were attenuated, as evidenced by lower viremia, decreased weight loss, and no mortality; in contrast to the NS1 mutant, the knockout of E glycosylation did not significantly affect neurovirulence. Mice immunized with the E mutant virus

developed a robust neutralizing antibody response and were completely protected from wild-type ZIKV challenge. In mosquitoes, the mutant virus exhibited diminished oral infectivity for the *Aedes aegypti* vector. Collectively, the results demonstrate that the E glycosylation is critical for ZIKV infection of mammalian and mosquito hosts. Additionally, a live-attenuated ZIKV strain encoding an NS1 protein without glycosylation (ZIKV-NS1-LAV) protected mice against transmission to the fetus. Vaccinated dams challenged subcutaneously with a heterologous ZIKV strain at embryo day 6 (E6) and evaluated at E13 showed markedly diminished levels of viral RNA in maternal, placental, and fetal tissues, which resulted in protection against placental damage and fetal demise. As live-attenuated vaccine platforms can restrict *in utero* transmission of ZIKV in mice, their continued development in humans to prevent congenital ZIKV syndrome seems warranted.

## TABLE OF CONTENTS

List of Tables .....	xi
List of Figures .....	xii
List of Abbreviations .....	xiv
<b>INTRODUCTION.....</b>	<b>17</b>
Chapter 1-Introduction .....	17
The Zika virus origin .....	17
Flaviviruses genome organization .....	18
Viral replication.....	19
N-linked Glycosylation .....	20
Glycosylated Proteins .....	20
Envelope .....	20
Nonstructural Protein 1 (NS1).....	21
N-LINKED GLYCOSYLATION IN FLAVIVIRUS .....	21
West Nile virus (WNV) .....	21
Dengue Virus (DENV) .....	22
Zika virus (ZIKV) .....	24
Vaccines .....	24
Zika Therapeutics .....	25
Conclusions and dissertation overview .....	25
<b>ZIKV GLYCOSYLATION.....</b>	<b>30</b>
Chapter 2- Materials and Methods.....	30
Cells and Antibodies.....	30
Viruses and cells.....	30
Plasmid construction .....	31
RNA Transcription, transfection, and indirect immunofluorescence assay (IFA) .....	31
Plaque assay .....	32
Virus multiplication kinetics .....	33



Western blots and glycosidase treatment.....	33
Quantitative reverse transcription PCR (qRT-PCR).....	34
Quantification of extra- and intracellular infectious virions.....	35
Mouse experiments .....	35
Virulence.....	35
Challenge studies .....	36
Measurement of viral burden .....	36
Infection and cytokine response in DCs.....	37
Neurovirulence on newborn CD-1 mice .....	37
Antibody neutralization assay .....	38
Infection of Mosquitoes with ZIKV.....	38
Viral RNA in situ hybridization (ISH) .....	39
Histology and immunohistochemistry .....	40
Quantification and statistical analysis.....	40
Illustrations.....	40
Chapter 3- Functional analysis of glycosylation of Zika virus envelope protein .....	42
Introduction .....	42
Results.....	44
Characterization of E glycosylation-knockout ZIKV in cell culture	44
Depletion of E glycosylation improves ZIKV attachment, virion assembly, and the infectivity of progeny virus in C6/36 cells	46
E N154Q mutation attenuates ZIKV in A129 mice .....	47
E glycosylation mutant ZIKV induces higher innate cytokine responses in dendritic cells (DCs) .....	48
E glycosylation does not significantly affect ZIKV neurovirulence	49
E N154Q mutation diminishes the ability of ZIKV to infect Aedes aegypti mosquitoes.....	49
Discussion.....	50
Chapter 4: Functional analysis of glycosylation of zika virus NS1 protein ....	66
Introduction .....	66
Results.....	67

Protective activity of a live-attenuated virus with mutations in NS1 .....	67
Vaccine protection against placental and fetal injury .....	70
Discussion.....	71
Conclusion .....	72
<b>DISCUSSION.....</b>	<b>86</b>
Chapter 5: Conclusion, Perspective, and Future Directions .....	86
Vita	107
References.....	94

## **List of Tables**

Table 2.1 Table of DNA Oligonucleotides for Cloning .....	41
---	----

## List of Figures

Figure 1.1 Flavivirus Genome.....	27
Figure 1.2 Flavivirus Life Cycle .....	28
Figure 1.3 N-linked Glycosylation .....	29
Figure 3.1 Characterization of N154Q mutant. ....	55
Figure 3.2 Effects of N154Q mutation on ZIKV life cycle in C6/36 cells. ....	57
Figure 3.3 Comparison of virulence between WT and N154Q in the A129 mice.....	59
Figure 3.4 Comparison of viral replication and innate cytokine responses in mouse DCs. ....	61
Figure 3.5 Comparison of neurovirulence between WT and N154Q in CD-1 mice.....	63
Figure 3.6. Infection of WT and N154Q in <i>Aedes aegypti</i> .....	64
Figure 3.S1. Analysis of thermostability, Related to Figure 3.1. ....	65
Figure 4.1 Development and characterization of a live-attenuated ZIKV vaccine with mutations in the NS1 gene .....	73
Figure 4.2 ZIKV-NS1-LAV protects pregnant C57BL/6 mice and their fetuses .....	75

Figure 4.3 ZIKV-NS1-LAV Vaccine Protects against Placental and Fetal Infection .....	77
Figure S4.1 Infectious Viral Titers in the Placenta and Fetal Heads, Related to Figure 2.....	78
Figure S4.2 ZIKV C38 Nano in Mosquitoes. Effects of Single Mutations in NS1 on ZIKV Infectivity and Pathogenesis, Related to Figure 1. ....	79
Figure S4.3. Sequencing Traces of NS1 Gene of Parental WT and ZIKV-NS1-LAV Viruses, Related to Figure 1 and 2. ....	81
Figure S4.4. Viral Burden in Different Organs of Parental and ZIKV-NS1-LAV Infected A129 Immunocompromised Mice, Related to Figure 1. ....	82
Figure S4.5. Mosquito Infectivity Assay, Related to Figure 1.....	83
Figure S4.6. Neutralizing Activity of Serum from ZIKV-NS1-LAV Vaccinated C57BL/6 Female Mice, Related to Figure 2. ....	84

## **List of Abbreviations**

BHK	baby hamster kidney
BLI	bioluminescent imaging
bp	base pair
C	capsid protein
CPE	cytopathic effects
CS	cyclization sequence
CZS	congenital Zika syndrome
DAR	downstream of AUG region
DC	dendritic cells
DENV1	dengue virus serotype 1
DENV2	dengue virus serotype 2
DENV3	dengue virus serotype 3
DENV4	dengue virus serotype 4
DMEM	Dulbecco's Modified Eagle Medium
DPBS	Dulbecco's phosphate buffered saline
E	envelope protein
ER	endoplasmic reticulum
FBS	fetal bovine serum
FFU	foci forming units
GBM	Glioblastoma
GBS	Guillain-Barré syndrome
GFP	green fluorescent protein
GSC	glioblastoma stem cell
HCV	hepatitis C virus

hpi	hours post infection
IFA	immunofluorescence assay
ISH	in situ hybridization
JEV	Japanese encephalitis virus
kb	kilobase
LAV	Live-Attenuated Vaccine
LOD	limit of detection
MIAF	mouse immune ascites fluid
MOI	multiplicity of infection
Nano	Nanoluciferase
NanoLuc	Nanoluciferase
NHP	non-human primates
NPC	neural progenitor cells
NSC	neural stem cells
NT50	neutralization titers
PBS	phosphate buffered saline
PCR	polymerase chain reaction
PIV	purified formalin inactivated virus
PGNaseF	Peptide N-Glycosidase F
prM	pre-membrane protein
PRNT	plaque reduction neutralization test
RLuc	Renilla luciferase
RT-PCR	reverse transcription-polymerase chain reaction
SL	stem loop
TBEV	tick-borne encephalitis virus
UAR	upstream of AUG region
UTR	untranslated region

VP	vesicle packets
WNV	West Nile virus
WT	wild type
YFV	yellow fever virus
YFV17D	yellow fever virus vaccine strain 17D
ZIKV	Zika virus



## **INTRODUCTION**

### **Chapter 1-Introduction<sup>1</sup>**

In 2015-2016, the little known Zika virus (ZIKV) caused an epidemic in which it became recognized as a unique human pathogen associated with a range of devastating congenital abnormalities collectively categorized as congenital Zika syndrome (CZS). In adults, the virus can trigger the autoimmune disorder Guillain-Barré syndrome (GBS), characterized by ascending paralysis. In February 2016, the World Health Organization (WHO) declared ZIKV to be a Public Health Emergency of International Concern. The global public health problem prompted academia, industry, and governments worldwide to initiate development of an effective vaccine to prevent another ZIKV epidemic that would put millions at risk. The development of reverse genetic systems for the study and manipulation of RNA viral genomes has revolutionized the field of virology, providing platforms for vaccine and antiviral development.

#### **THE ZIKA VIRUS ORIGIN**

ZIKV was initially isolated in 1947 in the Zika Forest of Uganda from a sentinel rhesus monkey [1]. Prior to a 2007 outbreak, ZIKV circulation was restricted to Africa and Asia, causing a limited number of human infections, with symptoms described as asymptomatic or mild [2]. The first major outbreak of ZIKV occurred in Micronesia in 2007. By 2013, the virus had spread to French Polynesia, where neurological complications like Guillain-Barré syndrome were first noted.

---

<sup>1</sup> Content of this chapter has been previously published: Fontes-Garfias, C. R.; Shi, P.-Y. Reverse genetic approaches for the development of Zika vaccines and therapeutics. *Current Opinion in Virology* 2020; 44, 7-15, doi: 10.1016/j.coviro.2020.05.002.

Subsequently, ZIKV disseminated to the Americas, where it was initially identified in the northeast of Brazil [3]. Startling reports showed an increase of children born with microcephaly in the areas affected by ZIKV. Soon thereafter, the virus was discovered in the amniotic fluid of pregnant women whose fetuses presented with ultrasound-detected microcephaly [4]. From 2015 to 2018, ZIKV spread rapidly; more than 800,000 human cases were reported in the Americas [5]. ZIKV is mainly transmitted through the bite of infected *Aedes aegypti* mosquitoes [6]; however, the virus can also be acquired through sexual contact, vertical transmission, blood transfusion, and organ transplantation [7]. During the 2015-2016 epidemic ZIKV exhibited an enhanced potential to infect millions of people, and despite the high rate of asymptomatic infections (~80%) [8], the devastating congenital syndrome associated with ZIKV infection has underscored the importance of countermeasure development [9]. Therefore, the creation of a safe and efficacious vaccine is urgently needed. Since the epidemic, a number of platforms have been rapidly used for ZIKV vaccine development, including DNA, RNA, viral vector, chimeric flavivirus, and live-attenuated vaccine platforms [10]. Among these technologies, advances like reverse genetic systems have led to a rapid research response to the ZIKV epidemic including the swift initiation of vaccine and therapeutic development [11, 12].

#### **FLAVIVIRUSES GENOME ORGANIZATION**

The *Flaviviridae* family, genus *Flavivirus*, includes several medically important pathogens that cause human disease, such as Zika virus (ZIKV), dengue virus (DENV), yellow fever virus (YFV), West Nile virus (WNV), Japanese

encephalitis virus (JEV), and tick-borne-encephalitis virus (TBEV) [13]. ZIKV emerged at a global level after being linked to microcephaly during the 2015-2016 epidemic in South America [1]. Flaviviruses have a single-stranded, positive-sense RNA genome that encodes three structural proteins (capsid [C], precursor membrane [prM], and envelope [E]) and seven nonstructural (NS1, NS2A, NS2B, NS3, NS4A, NS4B, and NS5) proteins (Figure 1.1). The structural proteins and viral genomic RNA form viral particles, while the nonstructural proteins are involved in replication, assembly, and immune evasion [14].

### **VIRAL REPLICATION**

The virus enters the host cell via receptor-mediated endocytosis. The structural E protein mediates the first step of the virus entry into a host cell by interacting with cell surface receptors and attachment factors [15]. The E protein leads to the fusion of the virus and cell membranes. The viral genome is then released into the cytoplasm where the translation occurs. Viral replication takes place in the replication complexes formed in the endoplasmic reticulum (ER). Virus assembly takes place on the ER surface, where structural proteins (C-PrM-E) and newly synthesized viral RNA forms immature viral particles [16]. The progeny virus travels from the ER to the Golgi apparatus inside a viral envelope that is derived from the ER membrane. Mature infectious particles form as they transit through the Golgi network where the pr is cleaved from the prM by a host protease, Furin, and mature viruses are released via exocytosis [17] (Figure 1.2). A brief overview of N-linked glycosylation and flavivirus glycosylated proteins follows.

## **N-LINKED GLYCOSYLATION**

Glycosylation is one of the most common post-translational modification of proteins, is the covalent attachment of carbohydrates at specific amino acid sequence motifs (N-X-S/T) (Figure 1.3). It is called N-linked because the oligosaccharide is transferred to the amide group of asparagine by oligosaccharyl transferase, forming an N-glycosidic bond [18]. Glycosylation can: Stabilize protein conformation, accelerate folding, promote secondary structures, reduce aggregation; it offers protection and plays a role in signaling [19]. Almost as soon as the protein enters the ER lumen, it is co-translationally modified and becomes glycosylated. Mannose residues are trimmed as the protein goes through the secretory pathway [19].

### **Glycosylated Proteins**

#### ***ENVELOPE***

Flavivirus E protein is responsible for binding cellular receptors, triggering endocytosis and entry of the virus. Notable receptors include DC-SIGN, TIM/TAM receptors, integrins, and heat shock proteins [16]. The M and E proteins are also among the most immunogenic flavivirus proteins and constitute the majority of the targets of the humoral immune response, including neutralizing epitopes [17]. The envelope (E) glycoprotein of flaviviruses interacts with host cell membrane receptors, facilitating the virus entering the cell via endocytosis. For this reason, mutations and post-translation modifications of the E protein can influence virulence, tropism, replication efficiency, and immune system response [19]. Flaviviruses in vitro studies have suggested that the glycosylation of E protein

plays a role in virion release [20], replication, and virus assembly [21]. Studies *in vivo* have shown the E glycoprotein is involved in neuroinvasiveness in mice models [22] [23], critical for virulence in A129 mice [24, 25], and required for mosquito vector transmission [24]. Lastly, the deglycosylation of the E protein has been proposed as a live-attenuated vaccine approach [26].

### **NONSTRUCTURAL PROTEIN 1 (NS1)**

The first non-structural flavivirus protein plays a number of roles in the virus life cycle. NS1 is present in cell-associated, cell-surface, and secreted forms [27]. NS1 forms a homodimer necessary for viral replication and it is also secreted as a hexamer and is involved in immune system evasion and pathogenesis. In most flavivirus the NS1 contains two N-linked glycosylation sites at positions 130 and 207. Obliteration of NS1 sites in WNV attenuates mouse neuroinvasiveness. It functions intracellularly as a dimer to assist in viral replication, in which it interacts with NS4A and NS4B to aid in membrane rearrangement. NS1 is also the only secreted protein in the flavivirus genome, and it has been reported to be involved in immune response [28].

## **N-LINKED GLYCOSYLATION IN FLAVIVIRUS**

### **West Nile virus (WNV)**

WNV is divided into two groups: lineage I and lineage II. Lineage I strains are responsible for major human outbreaks and are distributed worldwide. The majority of lineage I strains are involved in outbreaks are E glycosylated at position N154. Interestingly, few lineage II strains are glycosylated and are restricted to the African continent [29]. In several studies, the WNV E protein glycosylation was

required for efficient viral multiplication in C6/36, Vero and BHK cells [23] [30] [22] [26] [29] [21]. The decrease in infectivity in the WNV glycosylation-null mutant was attributed to less efficient viral replication [22], assembly [21], and viral secretion [29]. In another WNV study, the knockout of E N154 glycosylation did not affect viral replication in C6/36 cells [29] but significantly reduced viral transmission in *Culex* mosquitoes [31]. Additionally, in WNV the glycosylation of the E protein was identified as a neuroinvasive determinant in BALB/c and Swiss mice; therefore it could be a possible enhancer of neuroinvasion [22] [23, 26]. The E glycosylation mutant was shown to be attenuated for neurovirulence and neuroinvasiveness in Swiss mice. To study the effect on immunogenicity, surviving mice were challenged with WT virus. The results showed that the mutant viruses induced an immune response that protected the mice when challenged [23]. The deglycosylation of the E protein has been proposed as a live-attenuated vaccine approach due to the identification of neutralizing titers from glycosylation defective mutant immunized mice [26]. Lastly, human (293T, BHK, K562, Hela, and DCs) cell-derived WNV presented a higher infectivity in cells expressing DC-SIGNR than DC-SIGN receptors [32, 33]; the infection was dependent on the N-linked glycosylation of the E protein [33].

### **Dengue Virus (DENV)**

The DENV structural viral E protein has two glycosylation sites (at residues N67 and N153). Mutagenesis studies showed that N153Q mutation reduces viral replication in BHK (mammalian) and C6/36 (mosquito) cells, but does not affect viral replication in intrathoraxially injected mosquitoes [34]. Depletion of N67

glycosylation of E protein abolishes the ability of DENV-2 to produce infectious virus in mammalian cells, but not in mosquito cells [34, 35]. The ablation of the glycosylation site of the E protein reduced DENV infectivity in mammalian cells (Vero and BHK-21), but not in mosquito cells (C6/36) [20] [35]. In DENV the lack of glycosylation increased infectivity in C6/36 cells by affecting virion release [20].

DC-SIGN receptors are expressed on macrophages and immature dendritic cells (DCs) and bind to mannose residues [36]. Mammalian and mosquito cells synthesize N-glycans differently; virus grown in mammalian cells can present mannose and complex carbohydrates on their E protein while mosquito cells derived virus display high mannose residues [37]. DENV derived from mosquito (C6/36), and mammalian (Vero) cells were similarly effective in infecting DC-SIGN expressing human monocytes (U937) and immature DCs [38]. DENV binds both DC-SIGN and DC-SIGNR leading to viral entry [36, 38, 39]. DC-SIGNR receptors are expressed in endothelial cells, lymph nodes and liver, and preferably bind to complex glycans [35]. DENV Cryo-electron microscope structure showed that one DC-SIGN CDR monomer binds to two glycosylation sites at N67 of two neighboring E proteins in each icosahedral asymmetric unit [40]. Mutant viruses lacking the glycosylation site at position 67 in DENV-2 displayed reduced infectivity of DCs [35]. In the mosquito host soluble C-type lectins are critical for the attachment of WNV and DENV-2 [41, 42]. Secreted mosGCTL-1 lectin enhanced WNV infection in *Aedes* mosquitoes interacting with cell surface protein mosPTP-1 leading to viral attachment and entry [42], this interaction was not observed in DENV-2 with mosGCTL-1 but with mosGCTL-3 [41].

## **Zika virus (ZIKV)**

Phylogenetic analysis showed that several African ZIKV stains, like MR776a, contains a four-amino acid deletion spanning the N154 glycosylation site; this deletion might represent an adaptation when the original MR776a isolate was given approximately 148 passages in mouse brain [43]. Several other historical strains (e.g., Malaysian strain P6-740) also lack the glycosylation motif, whereas all the contemporary epidemic strains contained the E N154 glycosylation site [25].

## **VACCINES**

In the recent epidemics in Asia and the Americas, Zika virus infection has caused devastating disease, most notably Guillain-Barre syndrome in adults and congenital malformation in fetuses. Since 2016, a ZIKV vaccine remains a global health priority as shown by the continued progress in ZIKV vaccine development. Several vaccine candidates have advanced to clinical trials: DNA vaccines, modified RNA vaccines, purified formalin inactivated virus (PIV), and vectored vaccines [44-47]. However, an approved vaccine is still not available to prevent and/or treat ZIKV infection. Therefore, the urgency remains to develop safe, efficacious, and cost-effective vaccines to meet the unmet medical need. Reverse genetics technology has allowed for a rapid response to the ZIKV epidemic, assisting in areas like basic science research to understand ZIKV factors and their role in the viral infection cycle, as well as to advance the development of therapeutics and vaccines [11]. The generation of cDNA infectious clones has enabled rational engineering of ZIKV to develop various vaccine approaches [9, 17, 24, 48-51]. Additionally, the reporter, replicon, and reporter virus particles (RVP) systems have provided critical tools for basic and translational research to aid in the development of these vaccines, as well as therapeutics and diagnostics.



## **ZIKA THERAPEUTICS**

Although significant progress has been made towards ZIKV vaccine development, there is no licensed vaccine yet. This gap highlights the importance of developing therapeutics for ZIKV. Antiviral therapy could provide an important countermeasure to treat infected individuals, particularly in the case of pregnant women with fetuses at risk of congenital Zika syndrome [52].

## **CONCLUSIONS AND DISSERTATION OVERVIEW**

In Chapter 1, I am at giving an overview of the Zika virus and to highlight the importance of N-linked glycosylation. Chapter 2 cover the materials and methods. In Chapter 3 & 4 will focus in on two specific ZIKV proteins: the envelope and NS1 proteins, respectively. Glycosylation of viral proteins is targeted as an approach for the developing of much needed vaccine and to understand the impact in viral replication.

Studies from other flaviviruses have suggested that the N-linked glycosylation of the E protein is important for viral multiplication in mammalian and mosquito cells [23] [29] [35] [30] [22] [21]. The ablation of the glycosylation site of the E protein reduced DENV infectivity in mammalian cells (Vero and BHK-21), but not in mosquito cells (C6/36) [20] [35]. The E protein glycosylation was required for efficient growth of WNV in C6/36, Vero and BHK cells [23] [30] [22] [26] [29] [21]. In DENV the lack of glycosylation increased infectivity in C6/36 cells by affecting virion release [20]. The decrease in infectivity in the WNV glycosylation-null mutant was attributed to less efficient viral replication and assembly [21]. In WNV the E protein glycosylation was identified as a neuroinvasive determinant in

mice, a possible enhancer of neuroinvasion [22] [23], and its deglycosylation has been proposed as a live-attenuated vaccine approach [26]. DC-SIGN, AXL, and TIM-1 entry factors mediate ZIKV infection [15]. The mechanism of the E glycoprotein interaction with entry receptors is not entirely known. Studies in YF reported that elimination of the first glycosylation site of NS1 leads to reduction in neurovirulence. The lack of NS1 glycosylation, *in vitro*, reduced virus replication and NS1 secretion [26, 27, 53].

The information regarding the E & NS1 glycoproteins comes from studies in other flaviviruses, and can be translated to ZIKV. However, ZIKV can cause congenital disease and be sexually transmitted, and it is possible ZIKV could have unique mechanisms and cellular interactions. The dissertation investigates the role of glycosylation of the ZIKV E and NS1 proteins and its contribution to the infection cycle, pathogenesis, and vaccine development. We hypothesized that the glycosylation of the Envelope and/or NS1 proteins contribute to ZIKV infectivity and propose it does it by influencing stages of the virus life cycle, therefore the project focused to define the biological function of glycosylation in viral replication *in vitro* and pathogenesis *in vivo*.

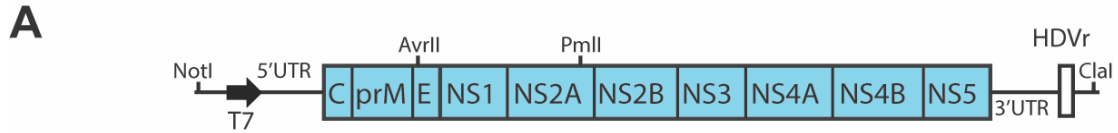


Figure 1.1 Flavivirus Genome.

A. General flavivirus genome organization. Three structural proteins: C-capsid, prM-pre-membrane, E-envelope, and seven nonstructural proteins. The structural proteins that form viral particles form viral particles while the nonstructural proteins help in replication, assembly, and evasion of the immune system. Restriction enzyme sites used for cloning are indicated. The drawing is not to scale.

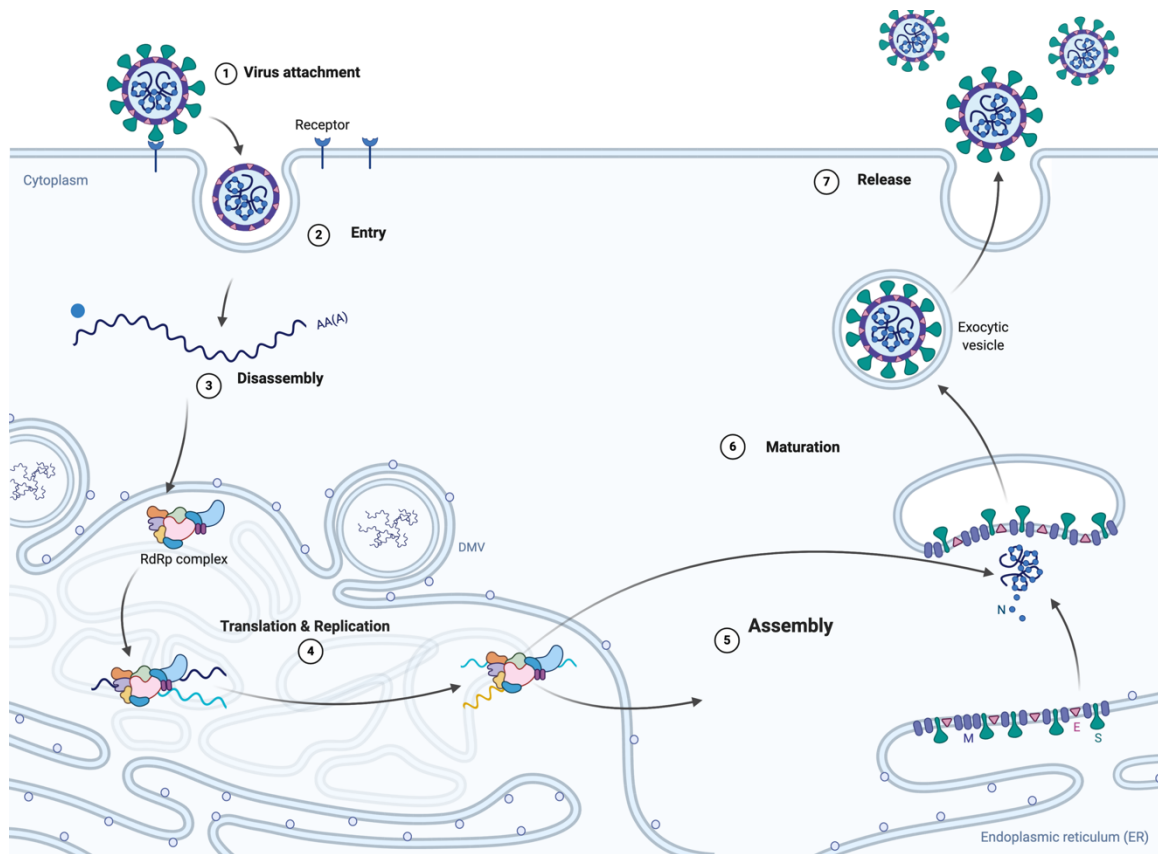


Figure 1.2 Flavivirus Life Cycle

The virus enters the host cell via receptor-mediated endocytosis. The structural E protein mediates the first step of the virus entry by interacting with cell surface receptors and attachment factors. The viral genome is then released into the cytoplasm where the translation occurs. Viral replication takes place in the replication complexes formed in the endoplasmic reticulum. Virus assembly takes place on the ER surface, where structural proteins and newly synthesized viral RNA forms immature viral particles. The progeny virus travels from the ER to the Golgi apparatus, the prM protein which is essential for viral particle formation is cleaved by a host furin protease into pr peptide and mature M. The virus exits the cell via exocytosis as mature viruses.

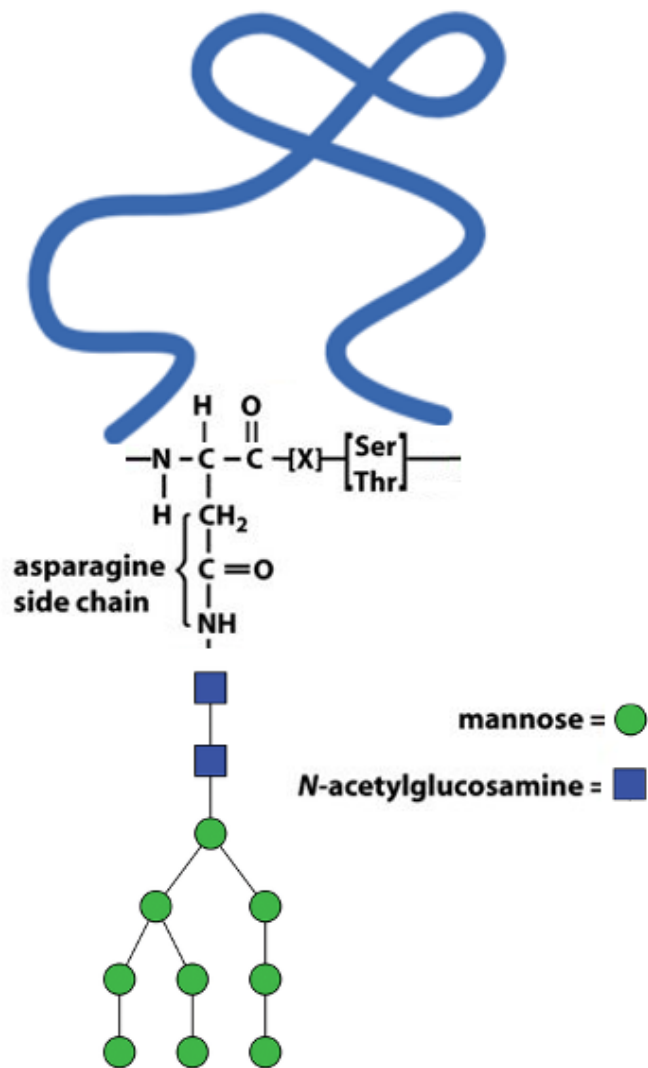


Figure 1.3 N-linked Glycosylation

Glycosylation is one of the most common intracellular modification of proteins, is the covalent attachment of carbohydrates at specific amino acid sequence motifs (N-X-S/T).

# **ZIKV GLYCOSYLATION**

## **Chapter 2- Materials and Methods**

### **CELLS AND ANTIBODIES**

Vero and C6/36 cells were cultured as previously reported [54]. The following antibodies were used in this study: a mouse monoclonal antibody (mAb) 4G2 cross-reactive with flavivirus E protein (ATCC), Rabbit Anti-Zika (African) Envelop DIII IgG (Alpha Diagnostic International), ZIKV-specific HMAF [hyper-immune ascitic fluid obtained from the World Reference Center of Emerging Viruses and Arboviruses (WRCEVA) at the University of Texas Medical Branch], anti-mouse IgG antibody labeled with horseradish peroxidase (KPL, Gaithersburg, MD), Anti-Rabbit IgG (H+L) Antibody Horseradish Peroxidase-labeled (KPL, Gaithersburg, MD), and goat anti-mouse IgG conjugated with Alexa Fluor®488 (Thermo Fisher Scientific). The ZIKV Cambodian strain FSS13025 (GenBank number KU955593.1) was generated from an infectious cDNA clone pFLZIKV as described previously [12].

### **VIRUSES AND CELLS.**

ZIKV strain Dakar 41519 (Senegal, 1984), FSS13025 (Cambodia, 2007), and PRVABC59 (Puerto Rico, 2015) were provided by the World Reference Center for Emerging Viruses and Arboviruses (University of Texas Medical Branch). To create a mouse-adapted more pathogenic variant of ZIKV Dakar 41519, it was passaged twice in Rag1<sup>-/-</sup> mice [55, 56]. Virus stocks were propagated in mycoplasma-free Vero cells and titrated by focus-forming (FFA) or plaque assays, as described previously [57, 58]. Experiments with ZIKV were conducted under

biosafety level 2 (BSL2) and A-BSL3 containment with Institutional Biosafety Committee approval.

## **PLASMID CONSTRUCTION**

The E N154Q mutations were introduced to the ZIKV full length cDNA infectious clone pFLZIKV [12]. A shuttle vector approach was used to amplify the DNA fragment between unique restriction sites NotI and AvrII using corresponding primers. Mutations were introduced to a fragment using QuickChange II XL Site-Directed Mutagenesis Kit (Agilent Technologies), then the fragment was digested and assembled to pFLZIKV. *E. coli* strain Top 10 (Invitrogen) was used to propagate the plasmids. The fragment and full-length plasmids were validated by Sanger DNA. All restriction enzymes were purchased from New England BioLabs (Ipswich, MA).

The NS1 single and double glycosylation mutations (N130Q, N207Q, and N130Q + S132A + N207Q + T209V) were introduced to the full-length ZIKV cDNA infectious clone pFLZIKV [12]. A shuttle vector spanning nucleotide position 1,466-3,881 (GenBank number KU955593.1) was used to introduce NS1 mutations by corresponding primers using QuickChange II XL Site-Directed Mutagenesis Kit (Agilent Technologies). The shuttle vector was digested and ligated to pFLZIKV using unique restriction enzyme sites AvrII and SphI. *E. coli* strain Top 10 cells (Invitrogen) were used to propagate the plasmids. The shuttle vector and full-length plasmids were validated by DNA sequencing. All restriction enzymes were purchased from New England BioLabs.

## **RNA TRANSCRIPTION, TRANSFECTION, AND INDIRECT IMMUNOFLUORESCENCE ASSAY (IFA)**

RNA transcription and transfection were performed as previously described [12]. For IFA, Vero cells transfected with viral RNA were seeded in 8-well Lab-Tek II chamber slide (Thermo Fisher Scientific, Waltham, MA). At indicated time points, cells were fixed in 100% methanol at -20°C for 15 min. After 1 h incubation in blocking buffer containing 1% FBS and 0.05% Tween-20 in PBS, the cells were treated with mouse monoclonal antibody (mAb) 4G2 for 1 h and washed three times with PBS (5 min for each wash). The cells were then incubated with Alexa Fluor® 488 goat anti-mouse IgG (Thermo Fisher Scientific) for 1 h in blocking buffer and washed three times with PBS. The cells were mounted in Vectashield® mounting medium with DAPI (4', 6-diamidino-2-phenylindole; Vector Laboratories, Inc.). Fluorescence images were observed under a fluorescence microscope (Olympus).

#### **PLAQUE ASSAY**

Twenty h prior infection, Vero cells were seeded into a 24 well plate cells ( $4 \times 10^5$  cells/well). Viral samples were 10-fold serially diluted six times in DMEM with 2% FBS and 1% penicillin/streptomycin. For each dilution, 100 µl sample was added to the Vero cells seeded in a 24 well plate; infections were executed in triplicates. After 1-hour incubation at 37°C, 0.5 ml methyl cellulose overlay containing 2% FBS and 1% penicillin/streptomycin was added to each well, and the plate was incubated at 37°C for 4 days. Following incubation, the methyl cellulose overlay, and the cells were fixed with 3.7% formaldehyde for 30 min at room temperature. After removing the fixative, the plate was stained with 1% crystal violet for 10 min. Visible plaques were counted, and viral titers (PFU/ml) were calculated.



## **VIRUS MULTIPLICATION KINETICS**

Vero ( $8 \times 10^5$  cells/well) and C6/36 cells ( $1.2 \times 10^6$  cells/well) were seeded in 6-well plates 24 h prior infection. Cells were inoculated with WT or N154Q virus at an MOI of 0.01; infections were executed in triplicates. Virus stocks were diluted in DMEM containing 2% FBS and 1% penicillin/streptomycin. One hundred  $\mu$ l of virus was added to each well of the 6-well plates. Cells were incubated for 1 h (5% CO<sub>2</sub> at 37°C for Vero cells and at 30°C for C6/36 cells), the inocula were removed, and cells were washed three times with PBS. Subsequently, 3 ml of fresh media containing 2% FBS and 1% penicillin/streptomycin, was added to each well. The plates were incubated for 5 days and supernatants were collected daily. Standard plaque assay on Vero cells was used to determine the replication curves following a protocol mentioned above.

## **WESTERN BLOTS AND GLYCOSIDASE TREATMENT**

Vero cells were seeded in T-175 flask ( $1.75 \times 10^7$  cells/flask), inoculated with virus at an MOI of 0.01, and incubated at 37°C until the cytopathogenic effect was observed. The infected cells were harvested, washed with cold PBS, and lysed with RIPA buffer. The lysed cells were placed on a Fisher Scientific™ Mini-Tube Rotator for a gentle agitation for 1-h at 4°C. The lysates were then centrifuged for 10 min at 15,000 rpm at 4°C, to remove cell debris. Lysate aliquots were treated with Peptide N-Glycosidase F (PGNase F) in accordance with the manufacturer's instructions (New England BioLabs, Inc.). Proteins were analyzed under denaturing conditions in 12% SDS-polyacrylamide gel electrophoresis (SDS-PAGE) and transferred using a Trans-Blot® Turbo™ Blotting System (Bio-Rad Laboratories) onto a polyvinylidene difluoride (PVDF) membrane. Blots were then blocked in TBST buffer (10 mM Tris-HCl, pH 7.5, 150 mM NaCl, and 0.1%

Tween 20) supplemented with 5% skim milk for 1 h, followed by probing with primary antibodies (1:2000 dilution) for 1 h at room temperature. After three washes with TBST buffer, the blots were incubated with goat anti-rabbit conjugated to HRP (1:5000 dilution) in TBST buffer with 5% milk for 1 h, followed by three washed with TBST buffer. Amersham™ ECL™ Prime Western Blotting detection reagent (GE Healthcare, Chicago, IL) was utilized to detect the antibodies.

### **QUANTITATIVE REVERSE TRANSCRIPTION PCR (qRT-PCR)**

Viral RNAs were extracted from the supernatant using QIAamp® viral RNA Mini Kit (Qiagen®), and intracellular total RNAs were purified using RNeasy® Mini Kit (Qiagen®). Extracted RNAs were eluted in 50 µl RNase-free water. ZIKV RNA copies were determined using a specific probe (5'-FAM/AGCCTACCT/ZEN/TGACAAGCAATCAGACACTCAA/3IABkFQ-3') and a primer set (ZIKV\_1193F: 5'-CCGCTGCCCAACACAAG-3'; ZIKV\_1269R: 5'-CCACTAACGTTCTTTTGCAGACAT-3'). The probe contains a 5'-FAM reporter dye, 3' IBFQ quencher, and internal ZEN quencher. Following manufacturer's instructions, 15- µl reactions of the QuantiTect Probe RT-PCR Kit (QIAGEN) and 1.5 µl RNA templates were used to performed qRT-PCR assays using the LightCycler® 480 System (Roche). In vitro transcribed full-length ZIKV RNA were used as RNA standard for RT-PCR quantification. The mRNA level of the housekeeping gene glyceraldehyde-3-phosphate dehydrogenase (GAPDH) was measured using an iTaq™ Universal SYBR® Green One-Step Kit (Bio-Rad) and primers: H\_GAPDH-F (5'-TGTTGCCATCAATGACCCCTT-3'), H\_GAPDH-R (5'-CTCCACGACGTACTCAGCG-3'), AD\_GADPH-F (5'-GGTATGGCTTTCCGTGTCCC-3'), and AD\_GADPH-R (5'-GCGGCTTCCTTGACCTTCTG-3').

## **QUANTIFICATION OF EXTRA- AND INTRACELLULAR INFECTIOUS VIRIONS**

At given time points, about 1 ml culture fluids were harvested and centrifuged at  $500 \times g$  for 5 min to remove cell debris prior to storage at  $-80^{\circ}\text{C}$ . Infected cells were washed three times with cold PBS to remove unbound virions. Cell surface-associated viruses were removed by a 3 min wash with cold alkaline-high-salt solution (1 M NaCl and 50 mM sodium bicarbonate, pH 9.5). After twice cold-PBS washes, the cells were detached using 0.25% Trypsin-EDTA (ThermoFisher Scientific) and suspended in 3 ml DMEM medium containing 2% FBS. Total cells were collected by centrifugation at  $1,000 \times g$  for 5 min. The cell pellets were resuspended in 250  $\mu\text{l}$  DMEM medium with 2% FBS. One hundred microliters of the cell suspensions were centrifuged at  $1,000 \times g$  for 5 min to pellet the cells; the pelleted cells were then used for intracellular viral RNA extraction. The remaining 150  $\mu\text{l}$  of cell suspensions were lysed using a single freeze-thaw cycle (frozen at  $-80^{\circ}\text{C}$  and thawed at  $37^{\circ}\text{C}$ ). Afterward, cellular debris was removed by centrifugation at  $3,200 \times g$  for 5 min at  $4^{\circ}\text{C}$ , and the supernatant was harvested for plaque assay to determine the intracellular infectivity.

## **MOUSE EXPERIMENTS**

### **Virulence**

All animal work was performed as approved by the UTMB Institutional Animal Care and Use Committee (IACUC). Virulence was determined by using three-week-old A129 mice, a model susceptible to ZIKV infection [59]. A129 mice were subcutaneously injected with  $10^4$  PFU of WT or E N154Q virus, five mice per group. PBS was used to dilute the virus stocks to the desired concentration. The

inoculum was back-titrated to verify the viral dose. Mock-infected mice were given PBS by the same route. Mice were monitored for weight loss and signs of disease daily. Mice were bled via retro-orbital sinus (RO), after being anesthetized every other day, to quantify the viremia using plaque assay on Vero cells. On day 28 post-immunization, mice were anesthetized and bled to measure neutralization antibody titers using a mCherry ZIKV infection assay. Mice were challenged on day 28 post infection with ZIKV WT FSS13025 with  $1 \times 10^5$  via intraperitoneal (I.P.) injection. On day 2 post-challenge, the mice were bled to measure viremia. Viral titers of sera and inoculum were determined by plaque assay on Vero cells as described above.

### **Challenge studies**

For challenge studies in A129 mice, immunized animals were inoculated subcutaneously with  $10^6$  PFU of ZIKV PRVABC59. Immunized WT C57BL/6 female were mated with naïve WT male mice; at embryonic age 5 (E5), pregnant dams were treated with a 2 mg injection of anti-Ifnar1. At E6, mice were inoculated with  $10^5$  FFU of mouse-adapted ZIKV-Dakar by subcutaneous injection in the footpad. All animals were sacrificed at E13 or term, and placentas, fetuses and maternal tissues were harvested.

### **Measurement of viral burden**

At E13 (seven days after ZIKV challenge), maternal blood was collected and organs from dams (brain and spleen) and fetuses (placenta and fetal head) were recovered. Organs were weighed and homogenized using a bead-beater apparatus (MagNA Lyser, Roche), and serum was prepared after coagulation and

centrifugation. Tissue samples and serum from ZIKV-infected mice were extracted with the RNeasy Mini Kit (Qiagen). ZIKV RNA levels were determined by TaqMan one-step quantitative reverse transcriptase PCR (qRT-PCR) on an ABI 7500 Fast Instrument using standard cycling conditions. Viral burden is expressed on a log<sub>10</sub> scale as viral RNA equivalents per gram or per milliliter after comparison with a standard curve produced using serial 5-fold dilutions of ZIKV RNA from known quantities of infectious virus. For ZIKV, the following primer sets were used: 1183F: 5'-CCACCAATGTTCTCTTGCAGACATATTG-3'; 1268R: 5'-TTCGGACAGCCGTTGTCCAACACAAG-3'; and probes (1213F): 5'-56-FAM/AGCCTACCT TGACAAGCAGTC/3IABkFQ-3'. With some samples, viral burden was determined by plaque assay on Vero cells [60].

### **Infection and cytokine response in DCs**

Bone-marrow derived DCs were generated as described previously [61]. Briefly, bone marrow cells from A129 mice were isolated and cultured for 6 days in RPMI-1640 supplemented with granulocyte-macrophage-colony stimulating factor, and interleukin-4 (Peprotech) to generate myeloid DC. Day 6-cultured DCs were infected with ZIKV at an MOI of 1. At day 1, 3, and 4 p.i., culture fluids were measured for infectious virus using plaque assays on Vero cells [17]. The infected cells were extracted for total intracellular RNA using Trizol (Invitrogen). The amounts of intracellular viral RNA and various cytokine RNAs were quantified using quantitative RT-PCR as reported previously [62].

### **Neurovirulence on newborn CD-1 mice**

Groups of 1-day-old outbred CD-1 mice (n=6 or 8) were injected with WT or N154Q viruses with ten-fold dilutions from 10,000 PFU to 100 PFU by the intracranial route. Mice were monitored daily for morbidity and mortality.

### **Antibody neutralization assay**

Neutralizing activity of mouse sera was assessed using a mCherry ZIKV infection assay. Sera were 2-fold serially diluted starting at 1:100 in DMEM with 2% FBS and 1% penicillin/streptomycin, then incubated with mCherry ZIKV at 37°C for 2 h. Antibody-virus complexes were added to pre-seeded Vero cells in 96-well plates. After 48 h post-infection, cells were visualized by fluorescence microscopy using Cytation 5 Cell Imaging Multi-Mode Reader (Biotek) to quantify the mCherry fluorescence-positive cells. The percentage of fluorescence-positive cells in the non-treatment controls was set at 100%. The fluorescence-positive cells from serum-treated wells were normalized to those of non-treatment controls. A four-parameter sigmoidal (logistic) model in the software GraphPad Prism 7 was used to calculate the neutralization titers (NT50).

### **Infection of Mosquitoes with ZIKV**

*Aedes aegypti* colony mosquitoes derived from Galveston, TX, were exposed for 30 min to artificial blood meals consisting of 1% (weight/vol) sucrose, 20% (vol/vol) FBS, 5 mM ATP, 33% (vol/vol) PBS-washed human blood cells (UTMB Blood Bank), and 33% (vol/vol) DMEM medium. The 1 ml-blood meal was combined with 1 ml virus and offered to cartons of *Ae. aegypti* in Hemotek 2-ml heated reservoirs (Discovery Workshops) covered with a mouse skin. The final viral load in the blood meals was  $1 \times 10^6$  PFU/ml. Engorged mosquitoes were

incubated at 28°C, 80% relative humidity on a 12:12 h light:dark cycle with ad libitum access to 10% sucrose solution for 7 days and then frozen at -20°C overnight. To assess infection, the whole body of each individual mosquito was homogenized (Retsch MM300 homogenizer, Retsch Inc., Newton, PA) in DMEM with 20% FBS and 250 µg/ml amphotericin B. The samples were then centrifuged for 10 min at 5,000 × rpm. Afterward, 50 µl supernatants were inoculated into 96-well plates containing Vero cells at 37°C and 5% CO<sub>2</sub> for 3 days. Cells were fixed with a mixture of ice-cold acetone and methanol (1:1) solution and immunostained as described previously [12]. The infection rate was calculated using the number of virus-positive mosquito bodies divided by the total number of engorged mosquitoes.

### **Viral RNA in situ hybridization (ISH)**

RNA ISH was performed with RNAscope 2.5 Brown (Advanced Cell Diagnostics) according to the manufacturer's instructions, and as previously described [56]. Paraformaldehyde-fixed paraffin-embedded tissue sections were incubated for 60 min at 60°C and deparaffinized in xylene. Endogenous peroxidases were quenched with H<sub>2</sub>O<sub>2</sub> for 10 min at room temperature. Slides were boiled for 15 min in RNAscope Target Retrieval Reagents and incubated for 30 min in RNAscope Protease Plus solution before probe hybridization. The probe targeting ZIKV RNA was designed and synthesized by Advanced Cell Diagnostics (Catalog no. 467771); specificity of ZIKV probe binding was confirmed by parallel hybridization of positive (Mm Ppib, Catalog no. 313911) and negative (dapB, Catalog no. 310043) control probes in sequential tissue sections. Tissues were counterstained with Gill's hematoxylin and visualized with standard bright-field microscopy (Nikon Eclipse E400).

## **Histology and immunohistochemistry**

Harvested placentas were fixed in 10% neutral buffered formalin at room temperature and embedded in paraffin. At least three placentas from different litters with the indicated treatments were sectioned and stained with hematoxylin and eosin to assess morphology. Surface area and thickness of placenta and different layers were measured using Image J software.

## **QUANTIFICATION AND STATISTICAL ANALYSIS**

All data were analyzed with GraphPad Prism software. Kaplan-Meier survival curves were analyzed by the log rank test, and weight losses were compared using two-way ANOVA with Bonferroni multiple comparison test. For neutralization antibody titers and viral burden analysis, the log<sub>10</sub> titers and levels of viral RNA were analyzed by a Mann-Whitney test or Kruskal-Wallis two-way ANOVA with a multiple comparisons correction. Fetal resorption rates were analyzed by a chi-square test. Paired antibody titer values were analyzed for differences by a Wilcoxon matched paired sign-rank test. Results were expressed as the mean  $\pm$  standard deviation (SD). A P value of <0.05 indicates statistically significant.

## **ILLUSTRATIONS**

Figures were created using Adobe Illustrator and BioRender.com



Table 2.1 Table of DNA Oligonucleotides for Cloning

Primer	Sequence (5'-3')
1183F	CCACCAATGTTCTCTTGCAGACATATTG
1268R	TTCGGACAGCCGTTGTCCAACACAAG
(1213F)	56-FAM/AGCCTACCT TGACAAGCAGTC/3IABkFQ
NotI-1466-F	tctgcggccgcTAGAGCGAAGGTTGAGATAAC
Clal-3881-C	cgaatcgatACACGAGGCCAAGGCCAGCAG
NS1-N130Q-F	AGGGCAGCAAAGACAcagAACAGCTTTGTCGTG
NS1-N130Q-R	CACGACAAAGCTGTTctgTGTCTTTGCTGCCCT
NS1-N207Q-F	ATTGAGAGTGAGAAGcagGACACATGGAGGCTG-
NS1-N207Q-R	CAGCCTCCATGTGTCTctgCTTCTCACTCTCAAT
NS1-130-132-F	AGGGCAGCAAAGACAcagAACgcgTTTGTCTGGATGGT
NS1-130-132-R	ACCATCCACGACAAAcgcGTTctgTGTCTTTGCTGCCCT
NS1-207-209-F	ATTGAGAGTGAGAAGcagGACggtTGGAGGCTGAAGAGG
NS1-207-209-F	ATTGAGAGTGAGAAGcagGACggtTGGAGGCTGAAGAGG
E-N154Q-F	AGTGGGATGATCGTTcagGATACAGGACATGAA
E-N154Q-R	TTCATGTCCTGTATCctgAACGATCATCCCACT
NS1-N130Q-F	AGGGCAGCAAAGACAcagAACAGCTTTGTCGTG
NS1-N130Q-R	CACGACAAAGCTGTTctgTGTCTTTGCTGCCCT
NS1-N207Q-F	ATTGAGAGTGAGAAGcagGACACATGGAGGCTG
NS1-N207Q-R	CAGCCTCCATGTGTCTctgCTTCTCACTCTCAAT
Zika-839V	GATTAGAGTCGAAAATTGGATATTC
Zika-1303V	GCAAAGGGAGCCTGGTGACATGCGC
XbaI-3950C	GCTCTAGAtATCGATttGGCCAAAGCAAACCATTTGATGGGAAC

## Chapter 3- Functional analysis of glycosylation of Zika virus envelope protein<sup>2</sup>

### INTRODUCTION

Zika virus (ZIKV) was originally isolated in 1947 from the Zika Forest of Uganda, and belongs to genus *Flavivirus* from family *Flaviviridae* [1]. Others flaviviruses, such as dengue (DENV), Yellow fever (YFV), West Nile (WNV), and Japanese encephalitis viruses (JEV), are medically important pathogens. About 80% of ZIKV infections are asymptomatic [63]. The recent epidemics have documented that ZIKV infections are associated with a broad range of devastating disorders comprising congenital Zika syndrome [64] as well as Guillain-Barré syndrome [63]. ZIKV is mainly transmitted by *Aedes* mosquitoes and is also transmitted through sexual and blood transfusion routes [7]. It is a public health priority to develop effective vaccines and therapeutics of ZIKV [65].

ZIKV has a positive, single-strand RNA genome of about 11,000 nucleotides that encode three structural proteins (capsid [C], precursor membrane [prM], and envelope [E]) and seven non-structural proteins (NS1, NS2A, NS2B, NS3, NS4A, NS4B, and NS5). The structural proteins along with genomic RNA form viral particles, while the nonstructural proteins are involved in replication, assembly, and evasion of the host immune system [66]. Flaviviruses enter the host cell via receptor-mediated endocytosis. The viral E protein first interacts with

---

<sup>2</sup> Contents of this chapter have been previously published: Fontes-Garfias, C. R.; Shan, C.; Luo, H.; Muruato A.; Medeiros, D. B.A.; Mays, E.; Xie, X.; Zou, J.; Roundy, C. M.; Wakamiya, M.; Rossi, S. L.; Wang, T.; Weaver, S.C.; Shi P-Y. Functional Analysis of Glycosylation of Zika Virus Envelope Protein. *Cell Reports* 2017; 21: 1180-1190. DOI: 10.1016/j.celrep.2017.10.016

cellular surface attachment factors and receptors [67]. The virions are then internalized through the endocytic pathway [68]. In the late endosome, low pH triggers a series of conformational changes of the E protein, leading to the fusion of viral and cellular membranes. After uncoating from nucleocapsids, the viral genome is released into the cytoplasm where translation occurs. Genomic replication takes place in the replication complexes in vesicle packets (VPs) formed in the endoplasmic reticulum (ER). Virus assembly takes place on the ER surface at sites juxtaposed to the VPs, where structural proteins packages the newly synthesized viral RNA to form immature virions that bud into the ER lumen [69]. Mature infectious virions form as they transit through the Golgi network where the pr segment is cleaved from the prM by host protease Furin. The mature virions are released from infected cells via exocytosis [70].

The flavivirus E protein is a major surface glycoprotein involved in modulating the viral infection cycle and eliciting antibody response [66]. The E protein of most flaviviruses is post-translationally modified by N-linked glycosylation at amino acid 153/154 within a highly conserved glycosylation motif of N-X-T/S at positions 154-156, indicating the biological importance of this modification; however, some flaviviruses isolates lack E glycosylation, suggesting that the function of E can be achieved without the N-linked glycan [71-75]. For the WNV E protein, glycosylation plays a critical role in neuroinvasiveness in mice [23, 76], but does not show any effect on infection of mosquitos; in cell culture, the E glycosylation knockout reduces WNV replication in mammalian BHK and avian QT6 cells, but does not affect viral replication in mosquito C6/36 cells [77]. For

DENV E protein, there are two glycosylation sites (at residues N67 and N153). Mutagenesis studies showed that N153Q mutation reduces viral replication in BHK and C6/36 cells, but does not affect viral replication in intrathoraxially injected mosquitoes [34]. Depletion of N67 glycosylation of E protein abolishes the ability of DENV-2 to produce infectious virus in mammalian cells, but not in mosquito cells [34, 35]. For ZIKV, phylogenetic analysis showed that the prototype African strain MR776a contains a four-amino acid deletion spanning the N154 glycosylation site (Figure 3.1A); this deletion might represent an adaptation when the original MR776a isolate was passaged in mouse brains for about 148 rounds [43]. Several other historical strains (e.g., Malaysian strain P6-740 in Figure 3.1A) also lack the glycosylation motif, whereas all the contemporary epidemic strains contained the E N154 glycosylation site. The biological function of ZIKV E glycosylation remains to be determined. The goal of this study was to characterize the role of E glycosylation in ZIKV replication in cell culture, virulence in mouse models, and infection of mosquito vector.

## **RESULTS**

### **Characterization of E glycosylation-knockout ZIKV in cell culture**

Sequence alignment showed that, except for the high passage strain MR776a and several other historical strains (e.g., Malaysian P6-740), the E proteins from almost all other ZIKV isolates (including all the contemporary epidemic strains) have a conserved N-linked glycosylation motif (N-X-T/S; Figure 3.1A). The glycan, linked to residue N154 (Figure 3.1B), is exposed on the surface of domain I of the E protein [78]. To study the function of E glycosylation, a mutation

encoding N154Q in E protein of Cambodian ZIKV strain FSS13025, a close relative of all strains from the Americas was engineered in to the infectious clone. The N154Q mutation was elected because the side chains of glutamine and asparagine have the same polarity and differ by only one carbon. Upon transfection into Vero cells, the WT and mutant genomic RNAs generated similar amounts of E-expressing cells on day 3 post-transfection (Figure 3.1C). Similar plaque morphologies were observed for the WT and N154Q viruses derived from the transfected cells (Figure 3.1D). Sequencing of the full genome of the N154Q virus confirmed the engineered mutation without reversion or other mutations (Figure 3.1E). Continuous passaging of the mutant virus for three rounds (3 days per round) in Vero cells did not change the engineered N154Q substitution.

To demonstrate the glycosylation status of the viral E protein, the infected cell lysates were treated with peptide N-glycosidase F (PNGase F), an enzyme that removes high mannose and complex carbohydrates. Western blotting showed that the PNGaseF treatment increased the mobility of the WT E protein; in contrast, the PNGaseF treatment did not change the mobility of the N154Q E protein, which migrated slightly faster than the WT E protein (Figure 3.1F). The result indicated that the E protein expressed from the N154Q virus was not glycosylated.

We compared the multiplication kinetics of the WT and mutant viruses on three cell lines derived from the African green monkey (Vero), baby hamster kidney (BHK), and *Ae. albopictus* mosquito (C6/36). The two viruses showed comparable multiplication kinetics on Vero and BHK cells (Figure 3.1G&H). In contrast, the mutant virus reproducibly generated about 10-fold more infectious progeny virus on C6/36 cells than the WT virus on day 1 post-infection (p.i.), whereas the WT virus generated equivalent and slightly higher viral titers than the mutant virus on days 2 and 3 p.i. (Figure 3.1I). Overall, the data suggested that depletion of E glycosylation affects the initial cycle of ZIKV replication in mosquito C6/36, but not

in mammalian Vero and BHK cells. It is not known if the WT virus caught up with the mutant virus in C6/36 cells on day 2 and 3 p.i., whereas the yield of mutant virus was about 10-fold higher than the WT virus on day 1 post-infection.

### **Depletion of E glycosylation improves ZIKV attachment, virion assembly, and the infectivity of progeny virus in C6/36 cells**

Since the E glycosylation mutant reproducibly generated more infectious virus on C6/36 cells on day 1 p.i. (Figure 3.1I), the effect of E glycosylation was examined on the early steps (cell attachment and entry) and late steps (virion assembly and release) of an infection cycle. For analyzing viral attachment and entry, C6/36 cells were incubated with equal amounts of infectious WT or E N154Q virus (MOI of 1) at 4°C for 1 h, allowing the viruses to attach to the cell surface without entering (Figure 3.2A). After 1 h incubation at 4°C, the cells from group I (Figure 3.2A) were washed with PBS to remove unattached virus, and the amounts of viruses that had attached to the cell surface were measured by quantitative RT-PCR; the mutant attached 1.8-fold more virus to cells than the WT virus did (Figure 3.2B). The cells from group II (Figure 3.2A) were further incubated at 30°C to initiate viral entry. At different time points, the infected cells were stringently washed with an alkaline high-salt solution to remove free virus as well as cell surface-associated virus, and the intracellular viral RNA was quantified using RT-PCR. In agreement with the attachment result, significantly higher levels of mutant viral RNA were detected than those of the WT viral RNA at 1.5 to 7 h .p.i. (Figure 3.2B). The results indicated that the E N154Q mutation enhanced virus attachment and/or entry on C6/36 cells.

For analyzing the effect of E N154Q mutation on virion assembly and progeny virus infectivity, C6/36 cells were infected with WT or mutant viruses at an

MOI of 1 (Figure 3.2C). The unattached viruses in inocula were removed at 1 h p.i. by three times washing with PBS. After incubating the infected cells at 30°C for 14 and 20 h, intracellular and extracellular levels of viral RNAs and infectious viruses were measured (Figure 3.2D-G). In all cases, the mutant virus generated more viral RNA and infectious virions than the WT virus. To measure the efficiency of intracellular virion assembly, the intracellular viral RNA/PFU ratios; the results showed that the intracellular RNA/PFU ratios derived from the WT virus were 12- and 4.5-fold higher than those derived from the mutant virus at 14 and 20 h p.i., respectively (Figure 3.2H), suggesting that the mutant virus was more efficient in intracellular virion assembly in C6/36 cells.

Next, the extracellular viral RNA/PFU ratios were calculated to estimate the infectivity of progeny viruses derived from the C6/36 cells. As summarized in Figure 3.2I, the extracellular RNA/PFU ratios derived from the WT virus were 1.5-fold greater than those derived from the mutant at both 14 and 20 h p.i., suggesting that the infectivity of WT progeny virus was lower. Altogether, the results indicated that glycosylation of E protein decreased viral attachment, virion assembly, and the infectivity of progeny virus in C6/36 cells. In DENV-2, depletion of E glycosylation was also shown to increase virus entry, but reduce virion release [20].

### **E N154Q mutation attenuates ZIKV in A129 mice**

The virulence and immunogenicity of the E N154Q mutant virus were evaluated in the A129 mice, an immune compromised *ifnar*<sup>-/-</sup> model for ZIKV infection [59]. Figure 3.3A outlines the experimental scheme. Three-week-old mice were infected with 10<sup>4</sup> PFU of WT or mutant virus via the subcutaneous route. The infected mice were measured for weight loss (Figure 3.3B), viremia (Figure 3.3C),

and mortality (Figure 3.3D). Compared with the PBS-inoculated control animals, no significant weight loss was observed in the mutant virus-infected mice, whereas the WT-infected animals exhibited significant weight loss (Figure 3.3B). Mice infected with the mutant generated 3,734- and 4,311-fold lower peak viremia on day 2 and 3 p.i., respectively, than those infected with the WT virus (Figure 3.3C). No mortality was observed in the mutant-infected mice, whereas 40% mortality was observed in the WT virus-infected animals (Figure 3.3D). Collectively, the results demonstrated that the E glycosylation knockout attenuated ZIKV in A129 mice. The observed attenuation was not due to the differences in thermostability or temperature sensitivity of the two viruses, as they exhibited similar thermostability and temperature sensitivity on Vero cells (Figure 3.7).

To test if immunization with E N154Q virus could protect mice from WT ZIKV infection, we measured the neutralizing antibody titers of the infected mice on day 28 p.i. and then challenged the animals with  $10^5$  PFU of ZIKV strain FSS13025 via the subcutaneous route. Comparable high levels of neutralizing titers were detected from the WT and mutant virus-infected animals (Figure 3.3E). No infectious virus was detected from either the WT or mutant virus-infected animals post challenge; in contrast, viremia of  $10^6$  PFU/ml was detected in the PBS-immunized control mice (Figure 3.3F). These results indicated that the E glycosylation knockout virus could elicit robust antibody response and protected mice from ZIKV challenge.

### **E glycosylation mutant ZIKV induces higher innate cytokine responses in dendritic cells (DCs)**

Mammalian DCs are one of the cell types that are first infected after an infectious mosquito bite. the abilities of WT and E N154Q viruses to replicate and



induce innate cytokine responses were compared in primary DCs. Bone marrow-derived DCs from A129 mice were infected with WT or mutant viruses at an MOI of 1. Extracellular viruses, intracellular viral RNAs, and intracellular mRNA levels of different cytokines were measured post-infection. The mutant virus produced more infectious virus and intracellular viral RNA than the WT virus on days 3 and 4 p.i. (Figure 3.4A & B). The mutant virus also induced significantly higher cytokine expression, including IFN- $\beta$ , IL-1 $\beta$ , and IL-6 (Figure 3.4C). These results suggested that the E N154Q ZIKV induced higher primary cytokine responses, which may in turn suppress viral replication in infected animals.

### **E glycosylation does not significantly affect ZIKV neurovirulence**

The neurovirulence of WT and E N154Q viruses were compared through intracranial injection of 1-day-old CD-1 outbred mice. As reported previously [79], neonates succumbed to WT ZIKV infection in a dose-responsive manner (Figure 3.5). Mice infected with E N154Q virus showed mortality rates similar to those infected with the WT virus. As a control, no death was observed in PBS-inoculated mice (Figure 3.5). The result suggested that E glycosylation did not significantly contribute to ZIKV neurovirulence.

### **E N154Q mutation diminishes the ability of ZIKV to infect *Aedes aegypti* mosquitoes**

the effect of E glycosylation on ZIKV infection of *Ae. aegypti*, the main urban vector, was examined. Mosquitoes derived from Galveston, Texas were fed on artificial human blood meals containing  $10^6$  PFU/ml of WT or mutant virus. On day 7 post-feeding, engorged mosquitos with similar blood meal sizes were analyzed for the presence of virus in the bodies to estimate viral infection rates. Consistent with previous findings [80], WT virus showed an infection rate of 48% (Figure 3.6). In contrast, only 4% of the mosquitoes fed on the mutant virus were infected. The results indicated that glycosylation of E protein was important for ZIKV to infect *Ae. aegypti*.

## DISCUSSION

Like other flaviviruses, the E protein from almost all ZIKV strains is glycosylated at amino acid N154. Because the life cycle of ZIKV alternates between mammalian and mosquito hosts, the role of E N154 glycosylation was investigated in viral replication in A129 mice and *Ae. aegypti* mosquitoes. Viral replication of WT and E glycosylation mutant viruses was also compared in mammalian and mosquito cell lines. Discrepant results were observed from the *in vitro* and *in vivo* experiments in both hosts. In mosquito derived cells, when infecting C6/36 cells, ZIKV E glycosylation negatively regulated viral attachment, virion assembly, and infectivity of progeny virus (Figure 3.2); in contrast, when *Ae. aegypti* imbibed blood meals spiked with a high level of virus, the glycosylation was found to be critical for ZIKV infection (Figure 3.6). In the *in vitro* mammalian models, the E glycosylation did not affect viral replication in BHK and Vero cells; however, knockout of E glycosylation significantly attenuated ZIKV in the A129

mouse model, as evidenced by reduced viremia, less weight loss, and no mortality (Figure 3.3B-D). Interestingly, E glycosylation depletion did not significantly affect the neurovirulence when the mutant virus was directly injected into the brains of newborn CD1 mice (Figure 3.5).

Flavivirus enters host cells via receptor-mediated endocytosis [66]. The carbohydrates on viral E protein function as an initial attachment molecule to host cells through C-type lectins, a family of host proteins with carbohydrate-binding activity. Previous studies showed that lectins from mammalian and mosquito hosts engage flavivirus E protein through two distinct mechanisms. In mammalian cells, lectin molecules such as DC-SIGN are associated with cytoplasmic membrane through their transmembrane domains [81]. When DENV infects DCs, it binds to DC-SIGN on cell surface, leading to subsequent interactions with cellular receptor(s) and viral entry [82]. Cryo-electron microscope structure show that DC-SIGN binds to two glycosylation sites at N67 of two neighboring E proteins in each icosahedral asymmetric unit [40]. It is conceivable that the E glycosylation-mediated flaviviral attachment may be dependent on the expression level of lectins on mammalian cell surface. This might explain the discrepancy of ZIKV replication in mammalian cell lines and in A129 mice. In support of this hypothesis, transient expression of DC-SIGN in HEK-293 cells enhanced WT ZIKV infection [67]. However, the result from DC infection (Figure 3.4) argues against the above hypothesis. Compared with the WT virus, the glycosylation mutant replicated more efficiently and induced greater innate cytokine responses in the DCs derived from the A129 mice (Figure 3.4). The greater initial cytokine response may in return

restrict viral replication, leading to attenuated viremia and no mortality in the mutant virus-infected A129 mice; in addition, the higher innate cytokine response in DCs could boost stronger adaptive immunity in mice, resulting in high levels of neutralizing antibodies and complete protection upon WT ZIKV challenge (Figure 3.3). However, it should be noted that our current results do not exclude other possibilities that may also contribute to the in vitro and in vivo discrepancy in mammalian hosts.

In the mosquito host, distinct C-type lectins modulate different flavivirus infections. C-type lectins mosGCTL-1 and mosGCTL-3 are critical for the attachment of WNV and DENV-2, respectively, to cellular surface in mosquitoes [41, 42]. In contrast to mammalian lectin DC-SIGN that are presented on cellular surface through their transmembrane domains, mosquito lectins are not directly associated with the cell surface. These soluble, cell-free lectins could interact with the glycan of flaviviral E proteins to form a lectin-virus complex, which could then bind to specific lectin-binding proteins located on the mosquito cell surface, leading to viral attachment and entry. For example, WNV binds to cell-free lectin mosGCTL-1 which subsequently interacts with cell surface protein mosPTP-1 in mosquito [41]. Intriguingly, mosPTP-1 cannot serve as a cellular surface receptor to bind the mosGCTL-3/DENV-2 complex, suggesting that, similar to the specificity of mosGCTLs for different flaviviruses, DENV-2 may employ a mosPTP-1 analog to mediate viral entry into mosquito cells [42]. The distinct mechanism of mosquito lectin-mediated viral attachment may also explain the discrepancy of our in vitro

and in vivo results. The amounts of cell-free lectins and their cell surface receptors may be different between C6/36 cell line and live mosquitoes.

Since the E glycosylation mutation attenuated ZIKV, its potential use for live-attenuated vaccine development was explored. A single-dose immunization of A129 mice with  $10^4$  PFU E N154Q virus elicited a robust neutralizing antibody response and fully prevented viremia upon WT ZIKV challenge. Although E N154Q virus was attenuated in A129 mice and in infecting *Ae. aegypti* mosquitoes, this safety profile is not as good as two recently reported, live-attenuated vaccine candidates: a 3'UTR deletion virus and NS1 glycosylation knockout virus [79, 83]. The latter two vaccine candidates did not cause any mortality after  $10^3$  PFU of vaccine viruses were injected intracranially into 1-day-old CD-1 mice, and no mosquitoes were infected after feeding on blood meals containing  $10^6$  PFU/ml of the vaccine candidate viruses. In contrast, mortality was observed in CD-1 mice infected with  $10^2$  PFU of E N154Q virus (Figure 3.5), and 4% of engorged mosquitoes were infected after blood meal feeding (Figure 3.6).

In summary, the results demonstrate the importance of E glycosylation for ZIKV infection in A129 mice and *Ae. aegypti* mosquitoes. Together with previous studies, the data support the conclusion that E glycosylation of various flaviviruses may function differently when the viruses alternate their infections between mammalian and mosquito hosts. Future studies are needed to further understand the selective advantages of the E glycosylation, particular in mammalian hosts.

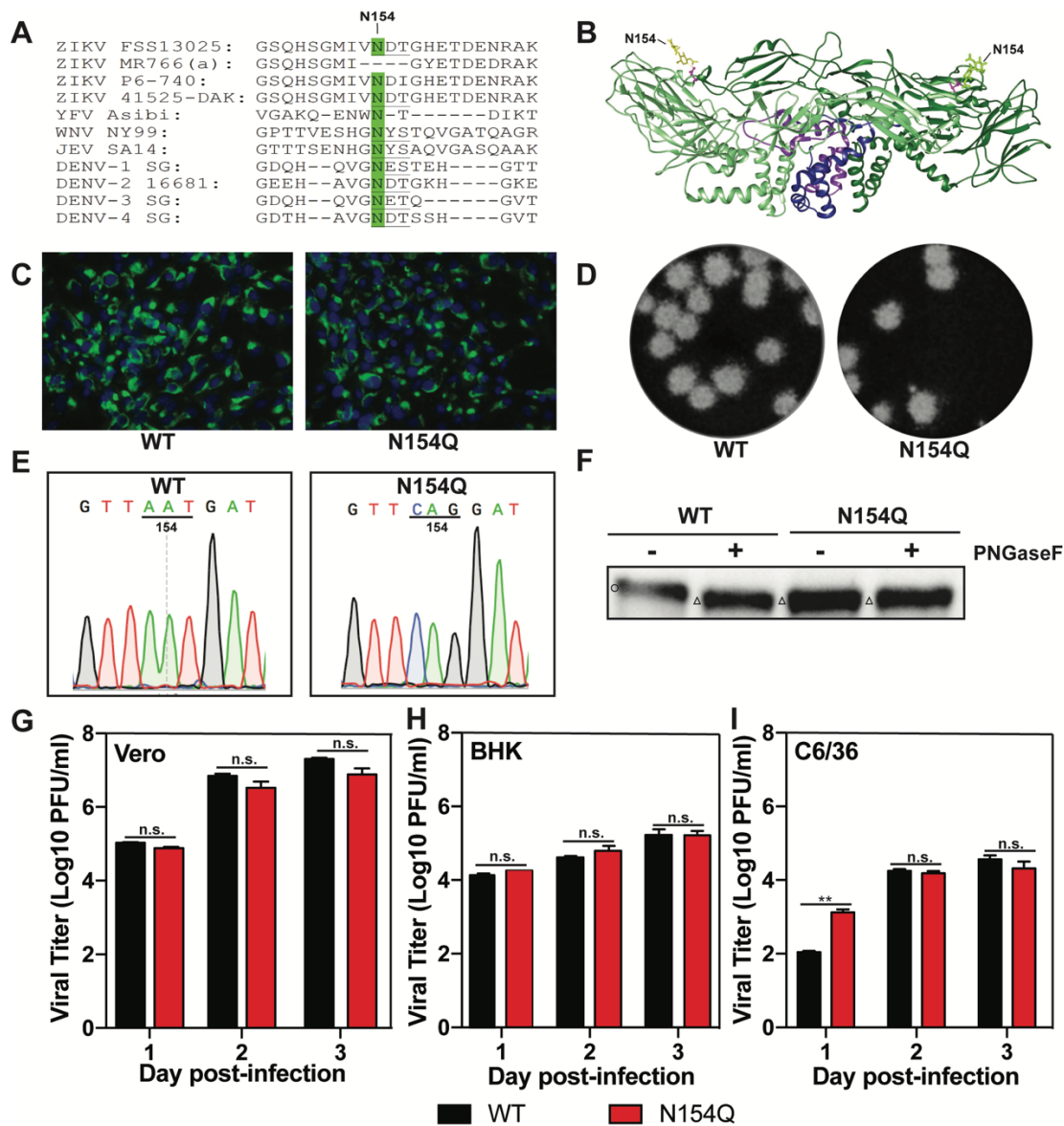


Figure 3.1 Characterization of N154Q mutant.

(A) Amino acid sequence alignment. The sequences of the E glycosylation site (positions 154-156) were compared among ZIKV strains FSS13025 (GeneBank number KU955593.1), MR776a (GeneBank number AY632535), P6-740 (GeneBank number KX377336.1), and 41525-DAK (GeneBank number KU955591.1), YFV strain Asibi (GeneBank number AY640589), WNV strain NY99 (GeneBank number DQ211652), JEV strain SA14 (GeneBank number D90194), DENV-1 strain SG/07K3640DK1/2008 (GeneBank number GQ398255), DENV-2 strain 16681 (GeneBank number NC\_001474), DENV-3 strain SG/05K863DK1/2005 (GeneBank number EU081190), and DENV-4 strain SG/06K2270DK1/2005 (GeneBank number GQ398256). The conserved glycosylation site at Asn 154 is highlighted in green. The glycosylation motif N-X-S/T is underlined. It should be noted that ZIKV P6-740 strain does not contain the conserved glycosylation motif of N-X-T/S. (B) 3-D dimer structure of ZIKV envelope protein. E protein dimer is shown in ribbon form; E protein monomers are colored in light and dark green and the transmembrane regions are colored in blue and purple. The N154 glycans on each monomer are labeled and shown projecting on the E protein surface (Protein Data Bank accession codes: 5IRE). (C) IFA of viral protein expression in cells transfected with WT and N154Q RNAs. Vero cells were electroporated with 10 µg of genome-length WT and N154Q RNA. On day 3 p.t., IFA was performed to examine viral E protein expression using a mouse mAb (4G2). Green and blue represent E protein and nuclei (stained with DAPI), respectively. (D) Plaque morphologies of WT and N154Q viruses. (E) Sequencing

traces of E gene of WT and N154Q viruses. (F) Endoglycosidase analyses of E protein. Proteins from WT and N154Q virus-infected Vero cells (MOI of 0.01) were analyzed by Western blot at 5 days post-infection. Lysates were treated with PNGase F for 1 h at 37°C. Western blot analysis of enzyme digested E was assessed by 12% SDS-PAGE under reducing condition using rabbit anti-E IgG as primary antibody. Symbols “O” and “Δ” indicate E proteins with and without glycosylation, respectively. (G-I) Comparison of growth kinetics of WT and N154Q viruses in Vero (G), BHK (H) and C6/36 (I) cells. Vero, BHK and C3/36 cells were infected with WT or N154Q virus at an MOI of 0.01. Viral titers were measured at indicated time points using plaque assays on Vero cells. Means and SDs from three independent replicates are shown. Statistics were performed using unpaired Student's t test; \*\*very significant ( $p < 0.01$ ).



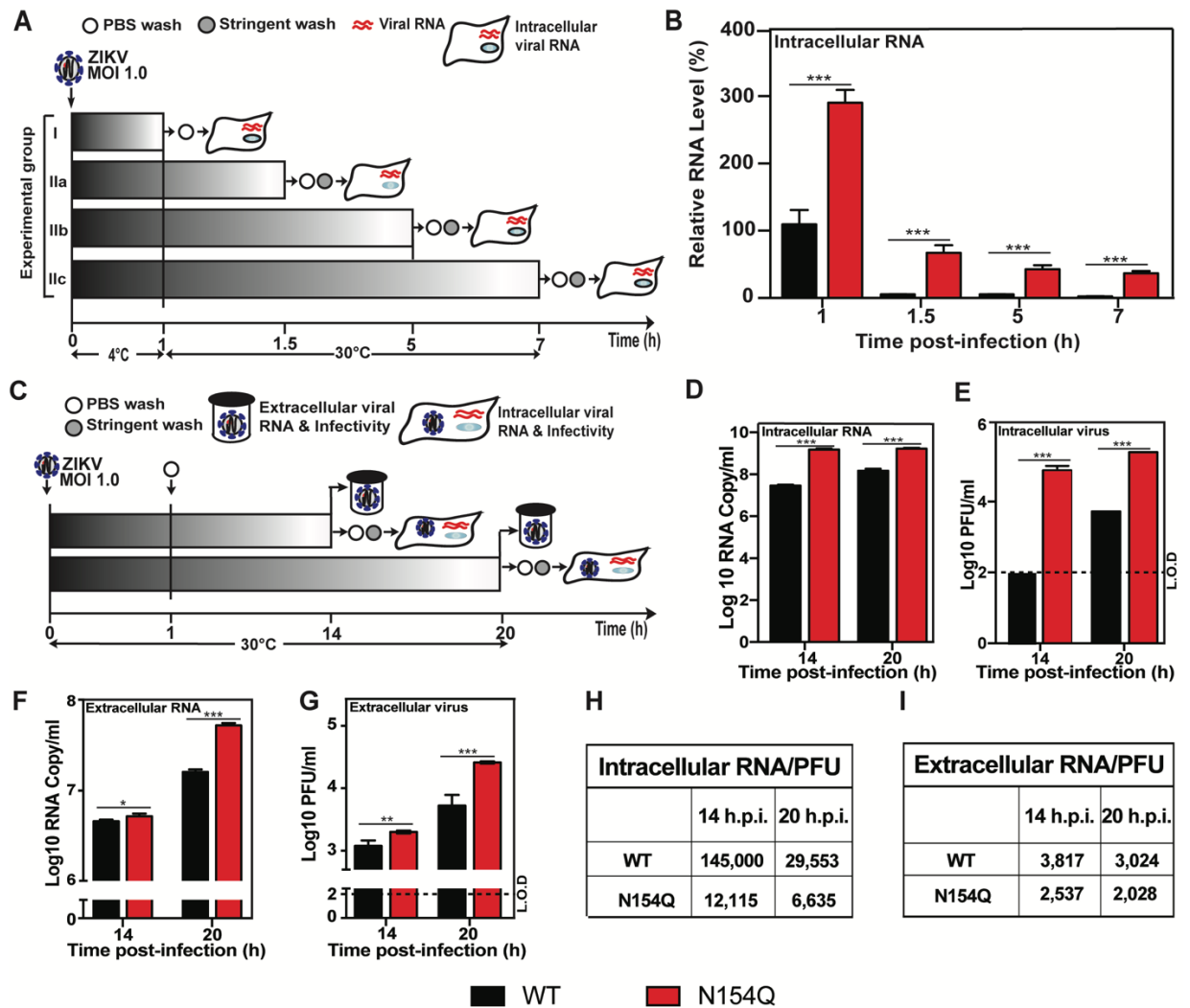


Figure 3.2 Effects of N154Q mutation on ZIKV life cycle in C6/36 cells.

(A) Overview of the experimental design to examine the virus attachment and entry. (B) Intracellular viral RNAs quantified at given time points from intracellular viral RNAs and GAPDH RNAs by qRT-PCR accordingly. The relative viral RNA levels were calculated by normalizing the viral RNAs at each time point to that of 1 h post-infection (set at 100%). Each data point represents the averaged relative RNA of three independent experiments. Statistics were performed using unpaired Student's t test; \*significant ( $p < 0.05$ ); \*\*very significant ( $p < 0.01$ ); \*\*\*extremely significant ( $p < 0.001$ ). (C) Overview of the experimental design to monitor a single

cycle of ZIKV infection. (D-E) C3/36 cells were infected with WT or N154Q virus at an MOI of 1.0. After infection, virus inoculums were removed, and cells were washed three times with PBS. To quantify intracellular viral RNAs at 14 and 20 h p.i., cells were further stringently washed with alkaline high-salt solution at the time the sample was harvested. Intracellular viral RNAs were measured by qRT-PCR and normalized using the cellular GAPDH RNA levels. Extracellular viral RNAs were determined by qRT-PCR, and infectious viruses were quantified by plaque assay. (D) Intracellular viral RNA. (E) Intracellular virus infectivity. (F) Extracellular RNA. (G) Extracellular virus infectivity. Each data point represents the average and standard deviations of three independent experiments. Statistics were performed using unpaired Student's t test; \*significant ( $p < 0.05$ ); \*\*very significant ( $p < 0.01$ ); \*\*\*extremely significant ( $p < 0.001$ ). (H-I) Intracellular and extracellular RNA Copy/PFU ratio.

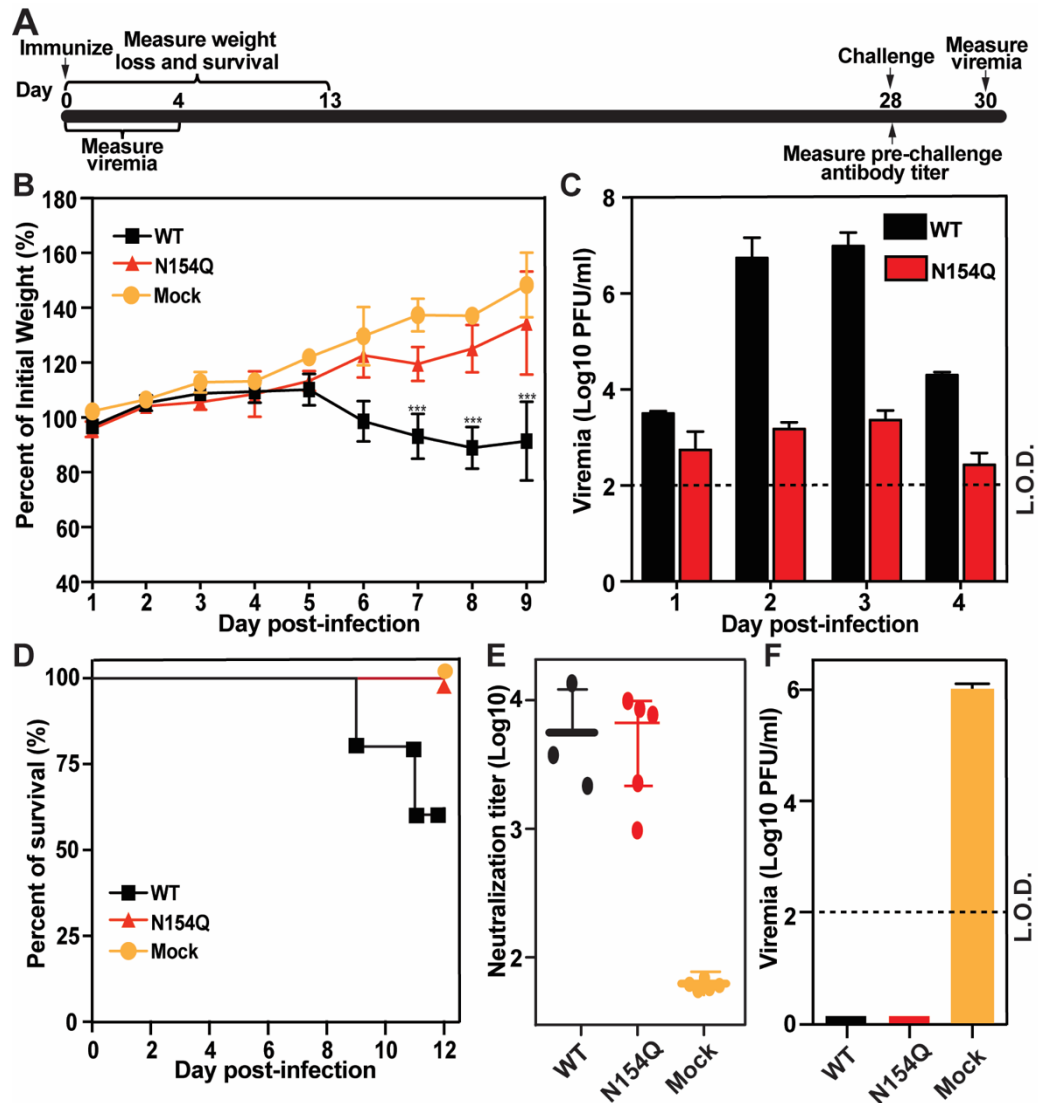


Figure 3.3 Comparison of virulence between WT and N154Q in the A129 mice.

Three-week old mice (5 mice per group) were infected with 10<sup>4</sup> PFU of WT or N154Q virus or PBS via sub-cutaneous injection. (A) Scheme of vaccination and challenge. (B) Mouse weight loss after infection with WT or N154Q virus. Mock or infected mice (n = 5 per group) were monitored for weight loss over the course of 9 days post-infection. A two-way ANOVA test was performed to evaluate the statistical significance of weight differences among WT and N154Q infected mice with mock group at each point. Error bar represent standard deviation. Symbols

\*\*\* indicate P values <0.001. (C) Mouse viremia after infection with WT and N154Q viruses. Viremia were quantified using plaque assay. The limit of detection (L.O.D.) for viremia is 100 PFU/ml. (D) Mortality for WT, N154Q and mock group. (E) Pre-challenge neutralization antibody titers. On day 28 p.i., mouse sera were measured for antibody neutralizing titers using a mCherry ZIKV infection assay. The expression of mCherry in infected Vero cells was analyzed by a fluorescent microscopy at 28 days post-infection. (F) Post-challenge viremia. On day 28 post-infection, mice were challenged with  $1 \times 10^5$  PFU parental virus (ZIKV strain FSS13025) via the I.P. route. Viremia on day 2 post-challenge was quantified using plaque assay. Error bar represent standard deviation.

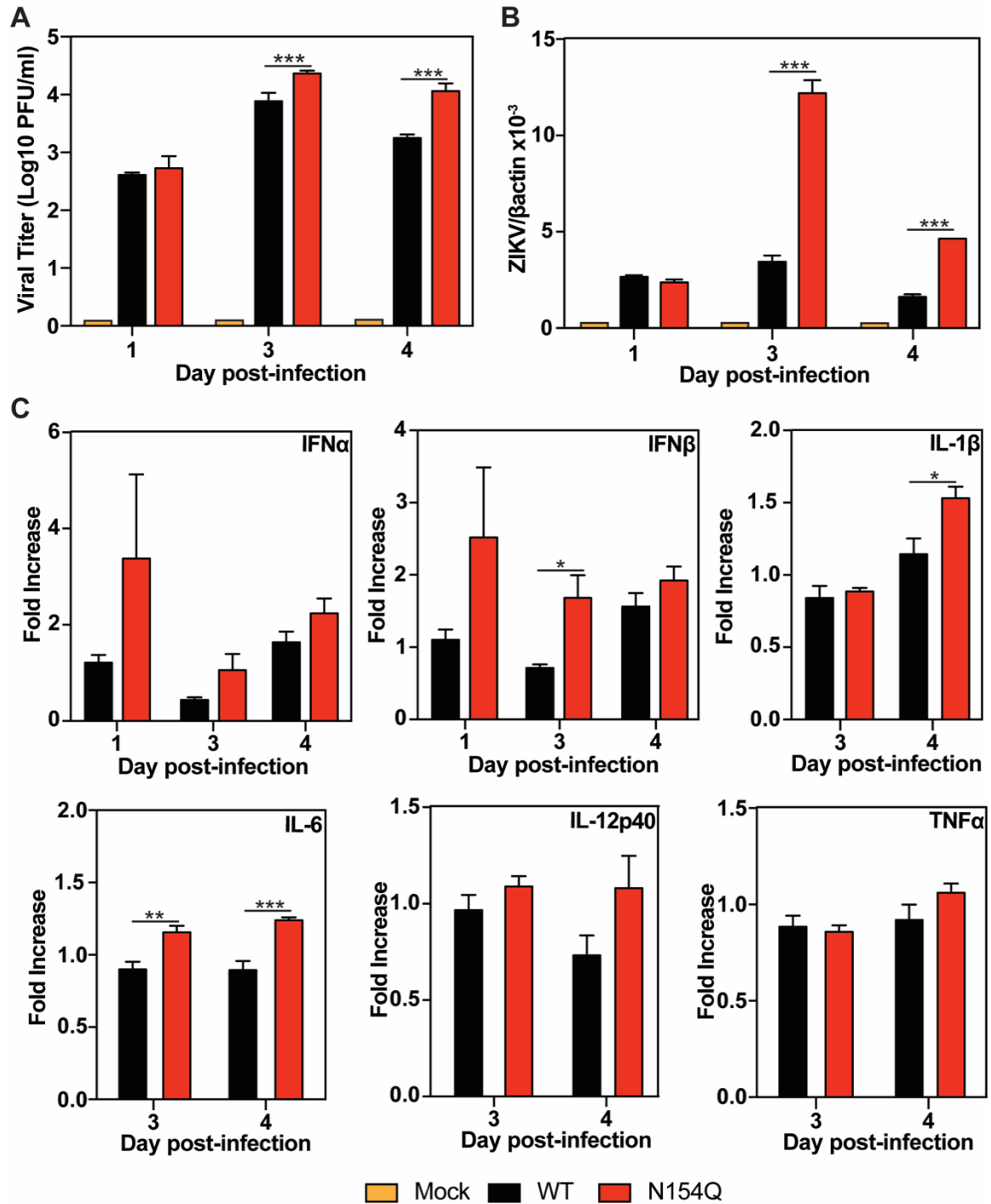


Figure 3.4 Comparison of viral replication and innate cytokine responses in mouse DCs.

Bone marrow-derived DCs from A129 mice were infected with WT or E N154Q mutant virus at an MOI of 1. At days 1, 3, and 4 p.i., extracellular infectious viruses

(A) and intracellular viral RNAs (B) were measured by plaque assay and quantitative RT-PCR, respectively. In addition, quantitative RT-PCR was used to quantify intracellular mRNA levels of different cytokines, including IFN $\alpha$ , IFN $\beta$ , IL-1 $\beta$ , IL-6, IL-12p40, and TNF $\alpha$  (C). Data are presented as means  $\pm$  SEM, n = 6. Statistical significance is presented as P < 0.05 (\*), P < 0.01 (\*\*), and P < 0.001 (\*\*\*) when compared to the WT ZIKV-infected group using unpaired t test.

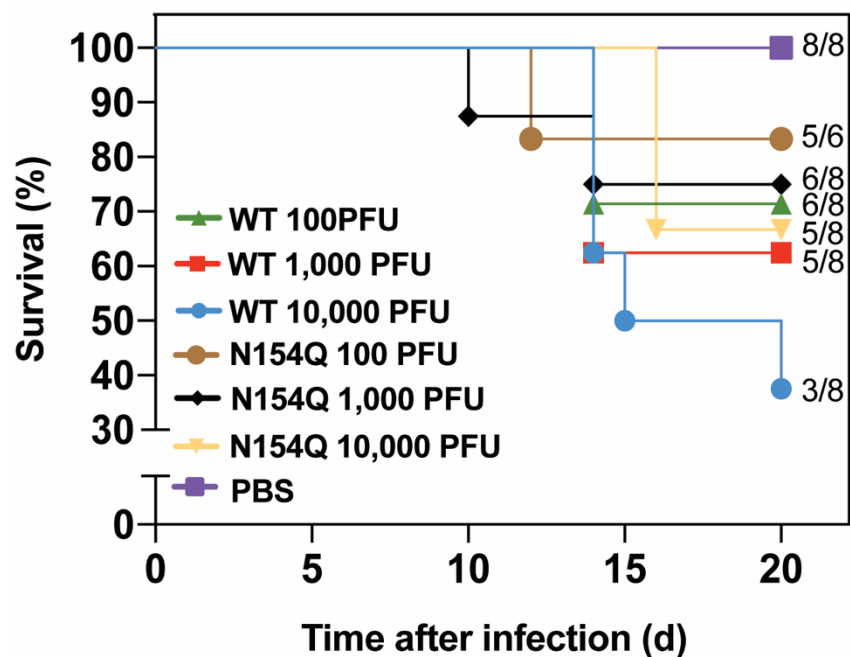


Figure 3.5 Comparison of neurovirulence between WT and N154Q in CD-1 mice.

One-day old mice (6 or 8 mice per group) were infected with 100 to 10,000 PFU of WT or N154Q virus via intra-cranial injection. Survival numbers and total number of infected mice were calculated. Survival percentages of infected mice are presented. No statistical significant difference was observed after performing Log-rank (Mantel-Cox) test to analyze the differences in survival between WT and N154Q.

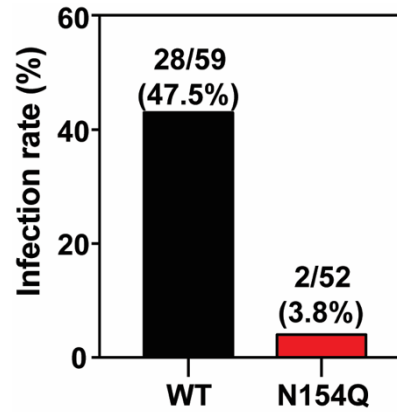


Figure 3.6. Infection of WT and N154Q in *Aedes aegypti*.

*Ae. aegypti* mosquitoes were fed with WT or N154Q virus on artificial blood meals for 30 minutes. On day 7 post-feeding, individual engorged, incubated mosquitoes were homogenized and infection was assayed by immunostaining of viral protein expression on inoculated Vero cells. The number of infected mosquitoes and total number of engorged mosquitoes are indicated.



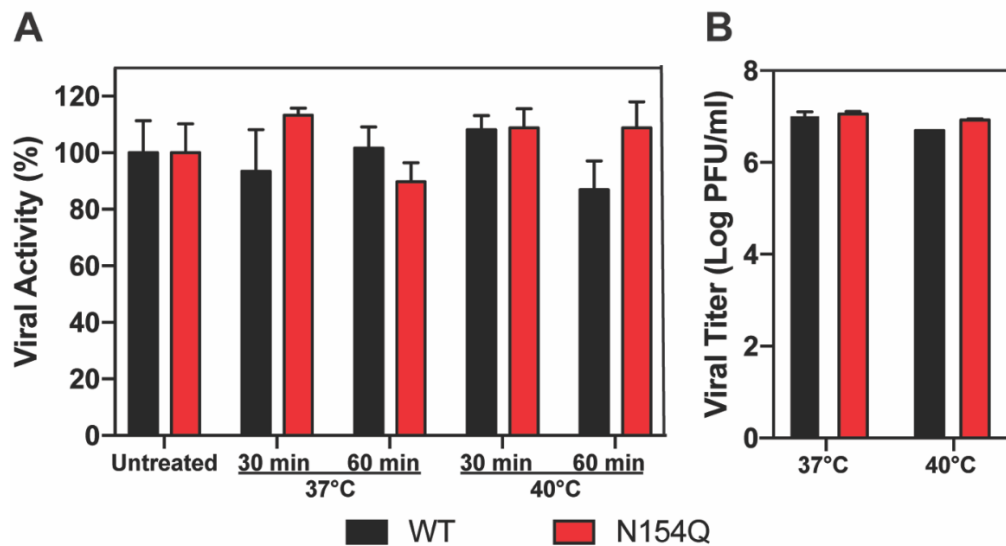


Figure 3.7. Analysis of thermostability, Related to Figure 3.1.

(A) and temperature sensitivity (B) of WT and N154Q viruses in Vero cells. (A) Thermostability analysis. WT and N154Q virus were pre-incubated at 37°C or 40°C for 30 min or 60 min. After incubation, viral titers in each sample were determined by plaque assay. The viral activity was calculated by normalizing the viral titers of treatment groups to those of untreated groups. A one-way ANOVA test was performed to analyze the statistical differences between each treatment group and corresponding un-treated group. (B) Temperature sensitivity analysis. For each virus, viral titers determined using standard plaque assay on two sets of WT or N154Q virus-infected Vero cells. Sets were incubated for 4 days at 37°C or 40°C, respectively. The average results of three experiments with standard deviations are presented.

## Chapter 4: Functional analysis of glycosylation of zika virus NS1 protein<sup>3</sup>

### INTRODUCTION

In a rapid response to the recent ZIKV epidemic, several groups have developed vaccine candidates based on subunit (prM-E or M-E DNA plasmid, adenovirus-vectored, or modified mRNA) or chemically inactivated whole-viral-particle approaches, all of which have elicited neutralizing antibodies that protect against ZIKV challenge in non-pregnant mice and non-human primates [84-89]. While several of these vaccine candidates have advanced to phase 1 clinical trials in humans [90], no study has established vaccine protection in the context of pregnancy.

In this chapter a newly engineered live-attenuated ZIKV vaccine (ZIKV-NS1-LAV) encoding mutations in the NS1 gene that abolished both N-linked glycosylation sites were evaluated for their ability to protect pregnant mice and their developing fetuses from ZIKV infection. Vaccination of wild-type (WT) female C57BL/6 mice with a single dose of ZIKV-NS1-LAV induced high-titers of neutralizing antibodies. Immunized female mice were mated to WT male sires and then infected at embryo day 6 (E6) with a pathogenic heterologous African ZIKV strain. Whereas placebo-immunized mice developed high titers of ZIKV in the maternal tissues, placenta, and fetal brain, those vaccinated with the ZIKV-NS1-LAV showed markedly diminished levels of virus in these tissues, with the majority of fetuses showing no evidence of infection.

---

<sup>3</sup> Content of this chapter has been previously published: Richner, J.M.\*; Jagger, B. W.\*; Shan, C.\*; Fontes, C. R.\*; Dowd, K. A.; Cao, B.; Himansu, S.; Caine, E. A.; Nunes, B. T. D.; Medeiros, D. B. A.; Muruato, A. E.; Foreman, B. M.; Luo, H.; Wang, T.; Barrett, A.D.; Weaver, S.C.; Vasconcelos, P. F. C.; Rossi, S. L.; Ciaramella, G.; Mysorekar, I. U.; Pierson, T. C.; Shi, P.-Y.; Diamond, M. S. Vaccine Mediated Protection Against Zika Virus-Induced Congenital Disease. *Cell* 2017; 170, 273-283.e12 DOI: 10.1016/j.cell.2017.06.040.

## RESULTS

### Protective activity of a live-attenuated virus with mutations in NS1

The ability of a live-attenuated ZIKV strain, to protect non-pregnant and pregnant mice from infection and disease was evaluated. Based on strategies for attenuating replication and virulence of other flaviviruses including YFV, DENV, and WNV flaviviruses [27, 28, 53, 91, 92], the N-linked glycosylation sites (N130Q and N207Q) of the NS1 gene of an Asian ZIKV (FSS13025, Cambodia, 2010) infectious cDNA clone [12] were mutated to create single or double glycosylation knockout variants (Figure 4.1A). Four amino-acid substitutions (N130Q/S132A, and N207Q/T209V) were engineered in the double glycosylation mutant to minimize reversion and enhance safety, as described for WNV [92]. Western blotting of virus infected cell lysates revealed the expected electrophoretic mobility shifts associated with loss of N-linked glycans on NS1 (Figure 4.1B). ZIKV with NS1 containing two glycosylation site mutations showed decreased plaque size and reduced replication in cell culture (Figures 4.1C–4.12E), with lesser attenuating effects of viruses containing one glycosylation mutation (Figures 4.5A and 4.5B). Although five serial passages of the double NS1 glycosylation mutant on Vero cells did not change the engineered substitutions as judged by consensus sequencing, an adaptive mutation (NS1-V134F) did emerge (Figure 4.6). The attenuation, immunogenicity, and protective activity of the NS1 glycosylation double knockout ZIKV (ZIKVNS1-LAV) was assessed in non-pregnant immunocompromised mice lacking type I interferon (IFN) signaling responses.

Three-week-old A129 male mice were divided into three groups, with each receiving a single subcutaneous inoculation of a placebo control (PBS), or  $10^4$  plaque forming units (PFU) of ZIKV-NS1-LAV, or parental WT ZIKV (Figure 4.1F). Morbidity, mortality, and viral burden were monitored over the first 2 weeks after inoculation. Whereas mice receiving the parental infectious clone-derived WT ZIKV developed substantial weight loss (Figure 4.1G), death (60% mortality; Figure 2H), and viremia ( $10^4$  to  $10^7$  PFU/ml at days 2 to 4 after infection; Figure 4.1I), ZIKV-NS1-LAV-inoculated mice sustained no weight loss or mortality, and developed less viremia ( $10^2$  to  $\sim 10^4$  PFU/ml) on corresponding days. Moreover, at days 6 and 10 post-infection, viral burden in the heart, lung, liver, spleen, kidney, muscle, brain, eye, and testis was substantially lower (100 to 1,000,000-fold) in A129 mice inoculated with ZIKV-NS1-LAV compared to WT ZIKV (Figure 4.7). In comparison, lower levels of attenuation in A129 mice were observed with the single glycosylation mutant (N130Q or N207Q) ZIKV strains (Figures 4.5C–4.5E). ZIKV-NS1-LAV also was attenuated in an intracranial inoculation model of outbred infant CD1 mice (50% lethal dose [LD50] of  $\sim 500$  PFU for WT ZIKV compared to  $>10,000$  PFU for ZIKV-NS1-LAV Figure 4.5F). Finally, we examined the ability of ZIKV-NS1-LAV to infect *Ae. aegypti* by feeding mosquitoes with artificial blood meals containing  $10^6$  FFU/ml of WT parental or ZIKV-NS1-LAV. On day 7 post-feeding, the WT virus infected 56% of the engorged mosquitoes. In contrast, none of the mosquitoes were infected by ZIKV-NS1-LAV (Figure 4.8), suggesting that the attenuated vaccine had markedly reduced ability to infect its principal urban mosquito.

At day 28, animals were phlebotomized for analysis of serum neutralizing antibody. A129 mice receiving either WT or ZIKV-NS1-LAV had strong neutralizing antibody responses, with EC50 values of  $\sim 1/5,000$  to  $1/7,000$  (Figure 4.1J). After challenge with  $10^6$  PFU of WT ZIKV PRVABC59 (Puerto Rico 2015), A129 mice receiving the placebo control sustained high levels ( $10^6$  to  $10^7$  PFU/ml) of viremia at day 2 (Figure 4.1K) compared to animals immunized with ZIKV-NS1-LAV or survivors of WT ZIKV infection, which had no detectable viremia at this time point.

Based on promising results in immunocompromised mice, the ZIKV-NS1-LAV platform was evaluated for protection during pregnancy (Figure 4.2A). Eight-week-old WT C57BL/6 female mice were vaccinated subcutaneously with a placebo control or  $10^5$  PFU of ZIKV-NS1-LAV; to facilitate transient replication of the attenuated strain in immunocompetent mice, we administered a single (0.5 mg) dose of anti-Ifnar1 monoclonal antibody 1 day prior to virus inoculation. No signs of illness (weight loss or change in activity) were observed after infection. Twenty-eight days later, animals were bled for serological analysis, which showed high titers of neutralizing antibodies with EC50 and EC90 values of  $1/25,000 \pm 2,000$  and  $1/5,800 \pm 600$ , respectively compared to the placebo control (Figure 4.2B–4.2D, and Figures 4.9A and 4.9B). One week later, immune female mice were mated with 12-week-old WT C57BL/6 male mice and monitored for vaginal plugs (Figure 4.2A). For the challenge studies, to facilitate ZIKV dissemination to the placenta, pregnant mice were administered 2 mgs of anti-Ifnar1 antibody at E5 1

day prior to infection (at E6) with  $10^5$  FFU of mouse-adapted ZIKV Dakar 41519. At E13, maternal and fetal organs were evaluated for tissue viral burden.

ZIKV-NS1-LAV conferred protection in the dams with reduced levels of virus in the spleen (~50,000-fold mean reduction, Figure 4.2E) and brain (~4,400-fold mean reduction, Figure 4.2F) compared to placebo-vaccinated animals. Placenta and fetal heads from ZIKV-NS1-LAV immunized dams also showed markedly lower levels of viral RNA (placenta, 276,000-fold mean reduction; fetal head, 20,000-fold mean reduction) than from placebo-immunized dams (Figure 4.2G and 4.2H). Indeed, 18 of 23 (78%) placentas and 19 of 23 (83%) fetal heads from ZIKVNS1-LAV immunized dams had viral RNA levels at or below the detection limit of the assay, suggesting that the vast majority of pregnant mice did not transmit ZIKV to their developing fetuses. Consistent with this observation, infectious virus was not recovered from the placentas or fetal heads from dams immunized with ZIKV-NS1-LAV (Figures 4.4A and 4.4B, n = 23).

### **Vaccine protection against placental and fetal injury**

The reduction in viral load mediated by ZIKV-NS1-LAV vaccine was associated with decreased damage of the placenta compared to placebo immunized dams. The ZIKV-NS1-LAV vaccines protected against ZIKV-induced placental insufficiency [60], as the total, labyrinth, and junctional areas of the placenta were greater than in infected animals receiving placebo vaccine (Figure 4.3A). In situ hybridization revealed an almost complete absence of viral RNA in the junctional zone and decidua of the placenta from animals immunized with

ZIKV-NS1-LAV as compared to placebo controls (Figure 4.3B). To determine the effects on fetal viability, we challenged ZIKV-NS1-LAV vaccinated and unvaccinated (placebo) dams and followed their pregnancies through term. Placebo-vaccinated dams had a lower rate of fetal viability compared to animals immunized with ZIKV-NS1-LAV (Figure 4.3C). Collectively, the virological and histopathological data suggests that immunization with prM-E mRNA LNP or ZIKV-NS1-LAV vaccines can reduce dissemination of ZIKV to the placenta, which substantially decreases the likelihood of placental infection and injury; this prevents vertical transmission and improves fetal outcome.

## DISCUSSION

This chapter has presented data to show a single dose of ZIKV-NS1-LAV given before pregnancy induced an immune response that protected against challenge during pregnancy with substantial reductions in maternal and placental viral titers, and prevention of transmission to the developing fetus. This attenuated ZIKV vaccine platform, which introduces four amino-acid substitutions and ten nucleotide changes to abolish the two N-linked glycosylation sites on the viral NS1 protein and prevent reversion, was based on a foundation of studies [27, 28, 53, 91] with other flaviviruses showing that such substitutions in NS1 are attenuating in cell culture, insects, and animals because of diminished replication rates, cytopathic effects, and immune evasion [93].

As modified mRNA and live-attenuated vaccine platforms can mitigate *in utero* transmission of ZIKV in mice, their development in humans for different target populations should be considered. Where safety concerns are greatest (e.g.,

females during childbearing years, immunocompromised, and those with certain co-morbidities), the non-replicating prM-E mRNA LNP subunit-based vaccine may have greatest utility and shortest pathway to licensure. In comparison, live-attenuated vaccines (e.g., ZIKV-NS1-LAV) administered before sexual debut may be associated with more rapid and long-term protection. Although the studies were focused on protection against transplacental transmission and fetal infection, the robust responses to the prM-E mRNA and ZIKV-NS1-LAV vaccines indicate they could diminish infection in other target populations and decrease the epidemic force of infection. Immunization of males may be important if the ZIKV-induced damage to the testes reported in mice [94-96] becomes apparent in humans or to prevent sexual transmission. An additional consideration is whether or not in the context of pregnancy the systemic immunity that is generated by vaccination is sufficient to prevent local vaginal infection and spread via organs of the reproductive tract that occurs during sexual transmission [97-99]. To address this issue, future studies should investigate vaccinated pregnant mice challenged via an intravaginal route.

## **CONCLUSION**

In summary, the live-attenuated vaccine platform generated sufficient immunity to protect against infection and disease in pregnant and non-pregnant mice. Based on these data, further evaluation of this platform to prevent congenital ZIKV syndrome in humans is warranted.



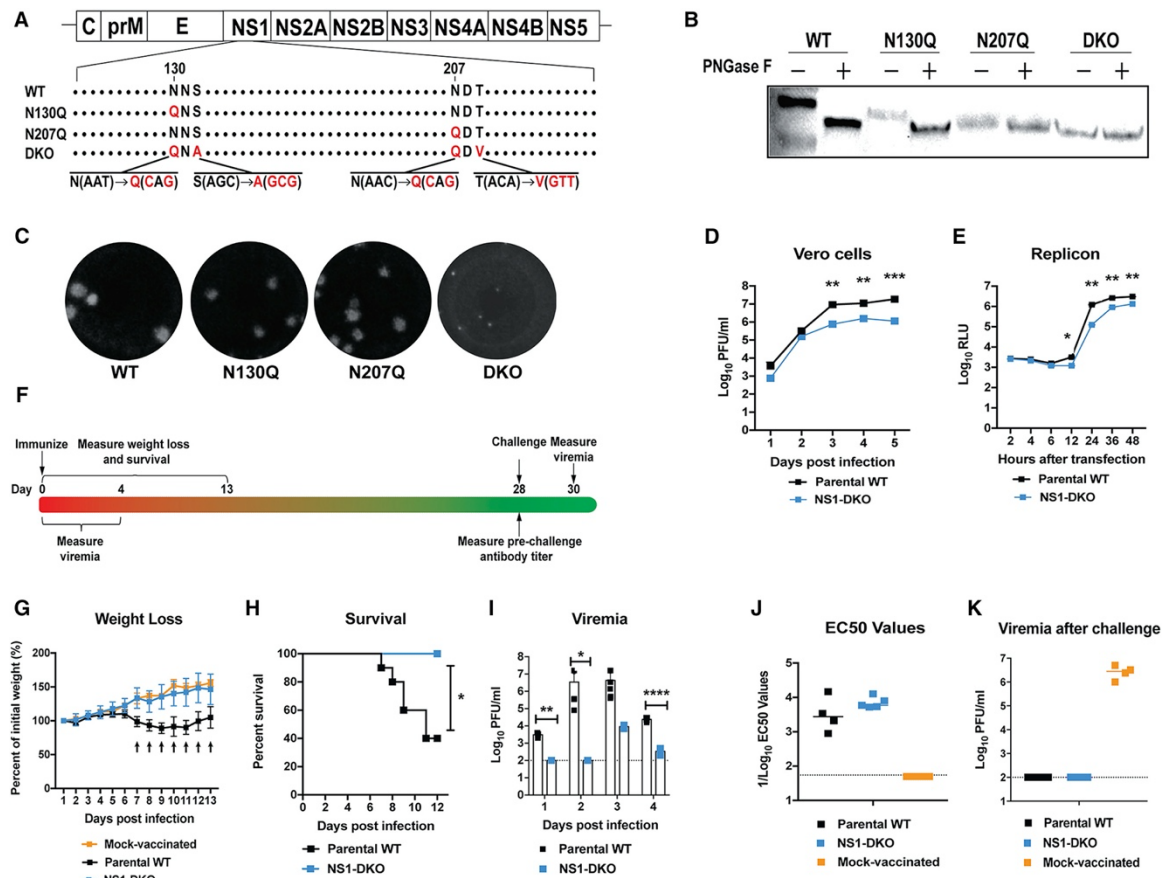


Figure 4.1 Development and characterization of a live-attenuated ZIKV vaccine with mutations in the NS1 gene

(A) Scheme of ZIKV genome with mutations in the NS1 gene. Mutated amino acids and their coding nucleotides are indicated in red. (B) Western blotting of lysates from Vero cells infected with parental WT, N130Q, N207Q, or N130Q+S132A+N207Q+T209V (DKO) ZIKV with an anti-NS1 antibody. Where indicated, PNGase F treatment was performed on lysates to remove N-linked glycans. Results are representative of several experiments. (C–E) Attenuated growth of ZIKV-NS1-LAV (DKO). Plaque assays (C), replication kinetics (D), and transient replicon (E) assays were performed in Vero cells. (D) Multi-step growth curves of parental WT and ZIKV-NS1-LAV in Vero cells. Results

are the average of two independent experiments, and the error bars indicate standard deviations (SD). (E) Replication of parental WT or ZIKV-NS1-LAV subgenomic replicons encoding a luciferase reporter gene after transfection of in vitro derived RNA into Vero cells. Results are the average of two independent experiments, and the error bars indicate SD. (F) Scheme of vaccination and challenge of 3-week-old *Ifnar1*<sup>-/-</sup> A129 male mice with parental and ZIKV-NS1-LAV. (G and H) Weight measurements (G) and mortality (H) over the first 2 weeks after immunization with mock vaccine (G) only, n = 4), parental WT (G), n = 5: (H), n = 10) or ZIKV-NS1-LAV (n = 5). Arrows (G) and asterisks (H) indicate statistically significant differences: ((G) Two-way ANOVA with Bonferroni multiple comparison test: day 7 and 8, \*\*\*p < 0.001; days 9–12, \*\*\*\*p < 0.0001; day 13, \*\*p < 0.01; (H) Log-rank test: \*p < 0.05). (I) Viremia measurements at days 1 through 4 after inoculation with parental (n = 5) and ZIKV-NS1-LAV (n = 3) as determined by plaque assay. Dotted line indicates limit of detection of assay. Asterisks indicate statistical significance (Mann-Whitney test: \*p < 0.05; \*\*p < 0.01; \*\*\*\*p < 0.0001). (J) Blood was collected at day 28 and analyzed for serum neutralizing activity. (K) A129 mice that were initially inoculated with placebo (mock-vaccinated) (n = 4), parental WT (n = 4) or ZIKV-NS1-LAV (n = 5) were challenged at day 30 with 10<sup>6</sup>PFU of ZIKV strain PRVABC59. At day 2 after challenge, viremia was measured.

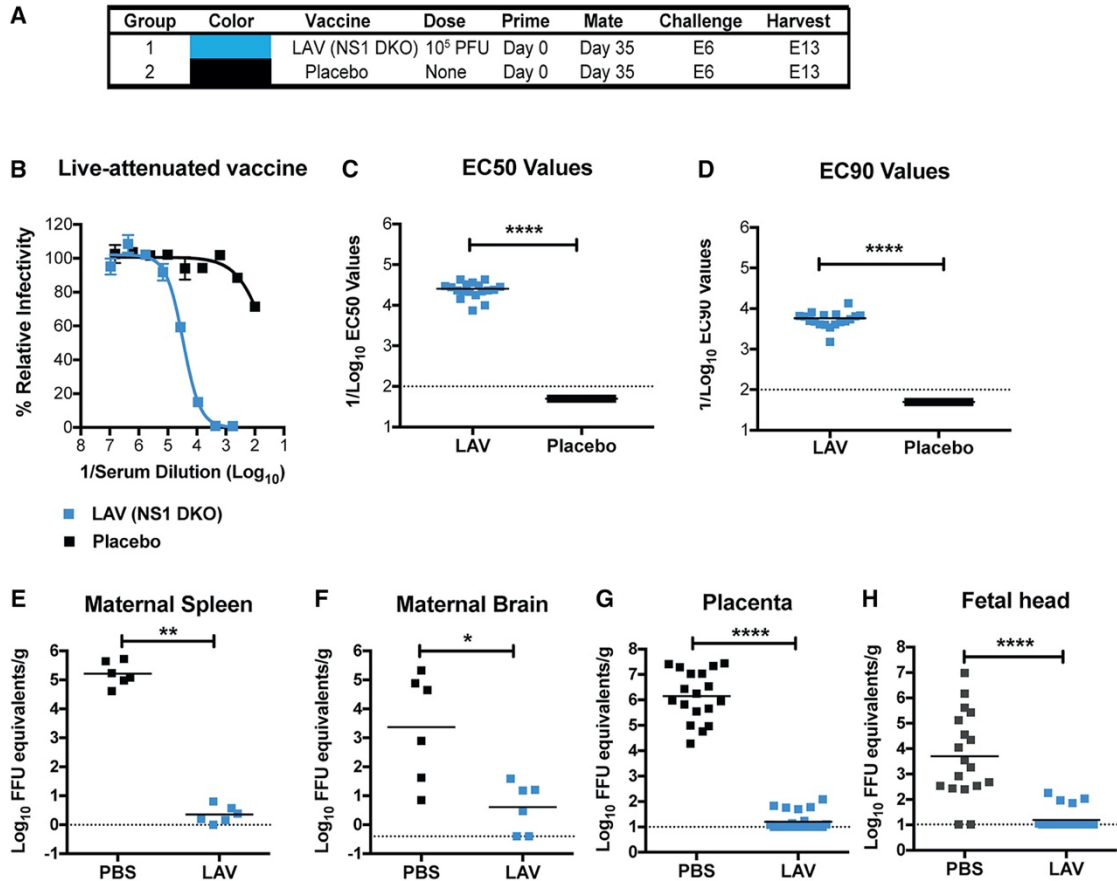


Figure 4.2 ZIKV-NS1-LAV protects pregnant C57BL/6 mice and their fetuses

Scheme of immunization of WT C57BL/6 female mice with 10<sup>5</sup> FFU of ZIKV-NS1-LAV (n = 18) or placebo (n = 11) control. One day prior to immunization, all mice were administered 0.5 mg of anti-Ifnar1. B. Serum was collected at day 28 and analyzed for neutralizing activity. Representative neutralization curves are shown. Error bars denote the standard deviation (SD) of triplicate technical replicates. C-D. EC50 (C) and EC90 (D) values were calculated for individual animals in each group (n = 20). The dashed lines indicate the limit of detection of the assay and data were analyzed (Mann-Whitney test: \*\*\*\*, P < 0.0001). E-H. At day 35, vaccinated female mice were mated with WT C57BL/6 males. A subset of the mice developed vaginal plugs (n = 6, PBS placebo; n = 6, ZIKV-NS1-LAV). Pregnant

mice were challenged with ZIKV at E13, animals were euthanized and maternal spleen (E), maternal brain (F), placenta (G), and fetal heads (H) were harvested and analyzed for levels of ZIKV RNA. The dashed line indicates the limit of detection of the assay and asterisks indicate significant differences (Mann-Whitney test: (\*,  $P < 0.05$ ; \*\*,  $P < 0.01$ ; \*\*\*\*,  $P < 0.0001$ ).

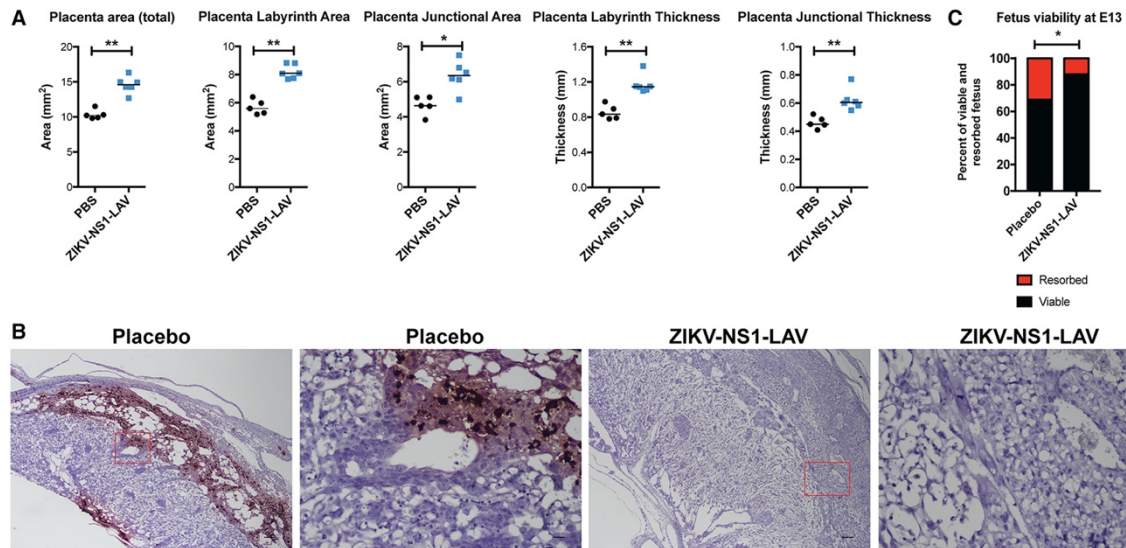


Figure 4.3 ZIKV-NS1-LAV Vaccine Protects against Placental and Fetal Infection

(A–C) Pregnant dams vaccinated with placebo or ZIKV-NS1-LAV were treated with anti-Ifnar1 and then inoculated with ZIKV-Dakar at E6 as described in Figure 1. (A). Measurements of thickness and indicated areas of placentas from placebo or ZIKV-NS1-LAV immunized mice after ZIKV challenge. Each symbol represents data from an individual placenta. Statistical significance was analyzed (Mann-Whitney test: \* $p < 0.05$ ; \*\* $p < 0.01$ ). (B) In situ hybridization. Low power (scale bar, 100  $\mu\text{m}$ ) and high power (scale bar, 20  $\mu\text{m}$ ) images are presented in sequence (indicated with a red box) from placebo or ZIKV-NS1-LAV immunized mice after ZIKV challenge. The images in panels are representative of three to four independent placentas from multiple dams. (C) Fetal resorption rates in placebo or ZIKV-NS1-LAV immunized dams after ZIKV challenge. Data are pooled from multiple dams in independent experiments and reflects the following number of fetuses ( $n = 32$  for placebo and  $n = 48$  for ZIKV-NS1-LAV). Significance for fetal survival was analyzed by the chi-square test (\* $p < 0.05$ ).

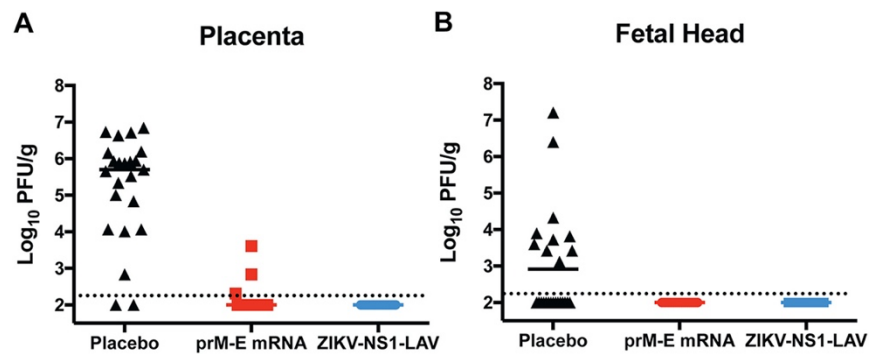


Figure 4.4 Infectious Viral Titers in the Placenta and Fetal Heads, Related to Figure 2.

(A and B) Placenta (A) and fetal heads (B) were collected at day 7 after challenge (E13) from placebo, prM-E mRNA LNP, and ZIKV-NS1-LAV immunized mice and tested for infectious virus by plaque assay. Dashed lines indicate limit of detection of the assays. Results are pooled from two independent biological experiments, and each symbol represents data from an individual placenta or fetus (n = 19 to 23). Bars indicate median values.

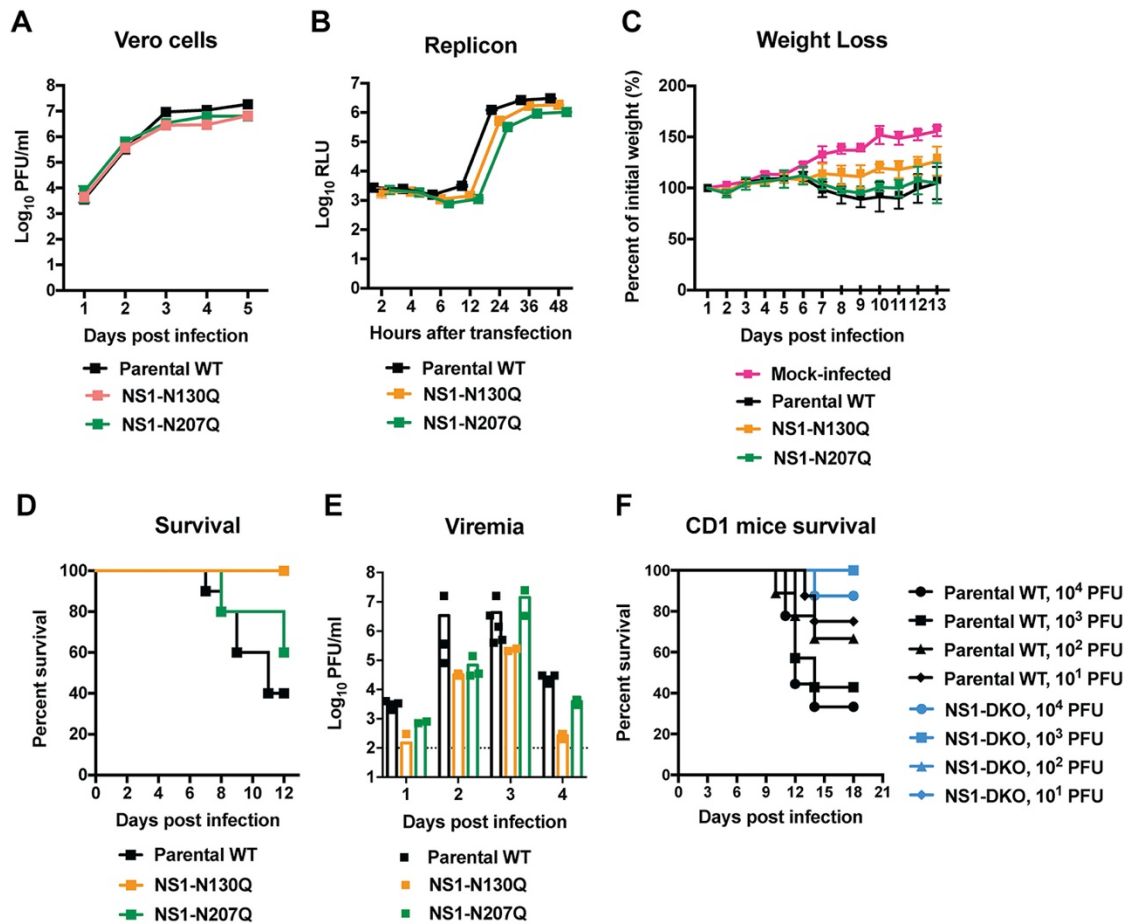


Figure 4.5 ZIKV C38 Nano in Mosquitoes. Effects of Single Mutations in NS1 on ZIKV Infectivity and Pathogenesis, Related to Figure 1.

(A and B) Growth of ZIKV-NS1-N130Q and ZIKV-NS1-N207Q in Vero cells. (A) Multi-step growth curve of parental and NS1 mutant ZIKV in Vero cells. Results are from two independent experiments, and the error bars indicate SD (B) Replication of parental WT and NS1 mutant ZIKV subgenomic replicons encoding a luciferase reporter gene after transfection of in vitro derived RNA into Vero cells. Results are from two independent experiments, and the error bars indicate SD. (C–E) Challenge of 3-week-old *Ifnar1*<sup>−/−</sup> A129 male mice with parental WT and NS1 mutant ZIKV. Weight measurements (C) and mortality (D) over the first

2 weeks after infection with mock infection (C) only, n = 4), parental WT (C), n = 5: (D), n = 10), ZIKV-NS1-N130Q (C), n = 5: (D), n = 5), or ZIKV-NS1-N207Q (C), n = 5: (D), n = 5). (E). Viremia measurements at days 1 through 4 after infection with parental (n = 5), ZIKV-NS1-N130Q (n = 3), and ZIKV-NS1-N207Q (n = 3) as determined by plaque assay. Dotted line indicates limit of detection of assay. For (A–E), the WT parental ZIKV data correspond to that shown in Figure 2, as the experiments were performed concurrently. (F) Survival studies in 1-day-old CD1 outbred mice. The indicated amounts of parental WT or ZIKV-NS1-LAV (DKO) (n = 6 to 9 mice per group) were inoculated via an intracranial route, and survival was monitored.



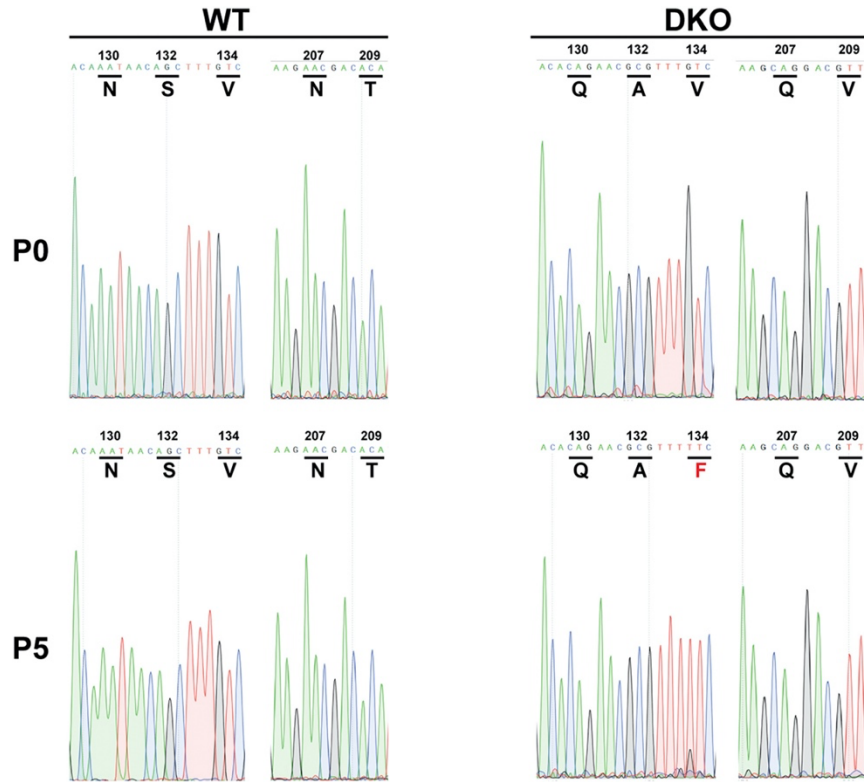


Figure 4.6. Sequencing Traces of NS1 Gene of Parental WT and ZIKV-NS1-LAV Viruses, Related to Figure 1 and 2.

Sequence tracings of relevant NS1 gene regions (amino acids 129–134, left; 206–209, right) for the parental WT and ZIKV-NS1-LAV (DKO) viruses at initial generation from an infectious cDNA clone (P0, top) or after five sequential passages in Vero cells (P5, bottom). Apart from the stability of the mutations that destroy the two N-linked glycosylation sites in NS1, ZIKV-NS1-LAV acquired a separate adaptive mutation (V134F) during passage (indicated in red), which enhanced growth in Vero cells.

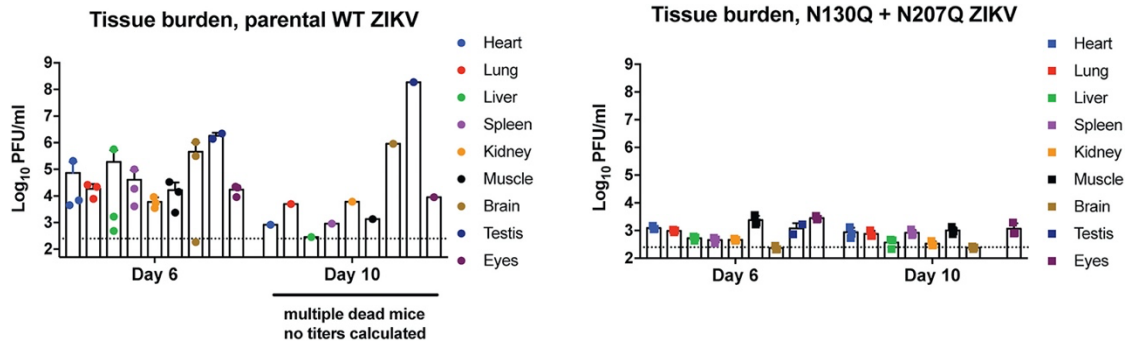


Figure 4.7. Viral Burden in Different Organs of Parental and ZIKV-NS1-LAV Infected A129 Immunocompromised Mice, Related to Figure 1.

Viral burden measurements in indicated tissues at days 6 and 10 after infection with parental (n = 3) and ZIKV-NS1-LAV (n = 3). Dotted line indicates limit of detection of assay.

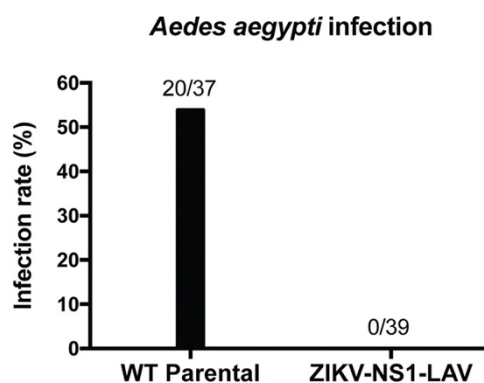


Figure 4.8. Mosquito Infectivity Assay, Related to Figure 1.

*Aedes aegypti* were fed with artificial blood-meals spiked with  $10^6$  FFU/ml of parental WT or ZIKV-NS1-LAV. Each engorged mosquito was homogenized on day 7 post-feeding and tested for viral infection using an immunofluorescence assay on Vero cells. The total number of engorged mosquitoes and infected mosquitoes are indicated above the bar graph.

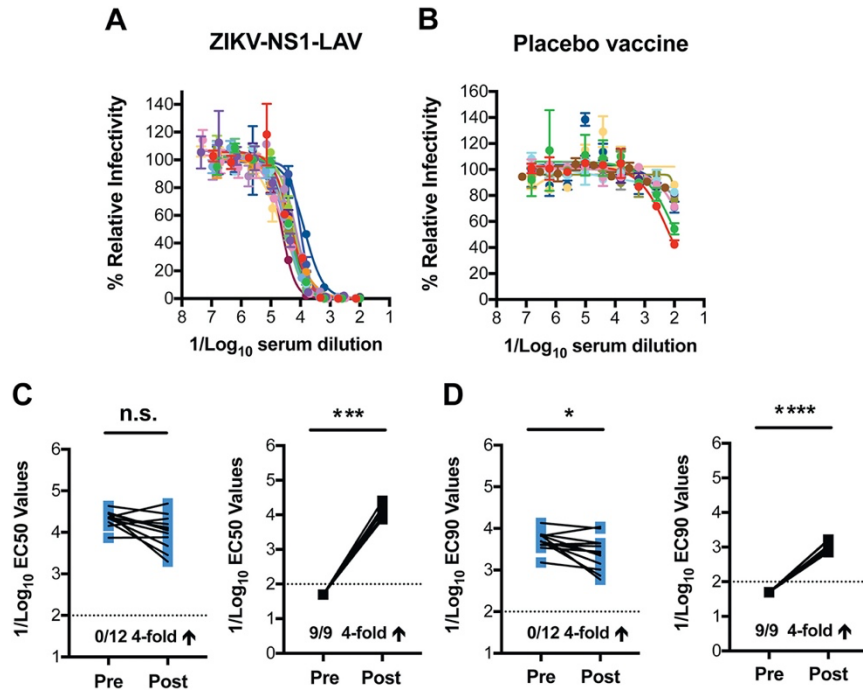


Figure 4.9. Neutralizing Activity of Serum from ZIKV-NS1-LAV Vaccinated C57BL/6 Female Mice, Related to Figure 2.

(A and B) Eight-week-old female C57BL/6 mice in each group were immunized with  $10^5$  PFU of ZIKV-NS1-LAV (Group 1, (A),  $n = 18$ ) or placebo (Group 2, (B),  $n = 11$ ). Serum was collected at day 28 post initial vaccination and analyzed for ZIKV neutralization activity by RVP assay. Each line represents the neutralization curve from an individual mouse. (C and D) Anamnestic neutralizing antibody response. Paired sera were collected from vaccinated animals (ZIKV-NS1-LAV or placebo) before (Pre) or 7 days after (Post) ZIKV challenge and analyzed for neutralizing activity (only pregnant animals shown). EC50 (C) and EC90 (D) values were analyzed for differences by a Wilcoxon matched paired sign-rank test (n.s., not significant; \* $p < 0.05$ ; \*\* $p < 0.01$ ). Indicated at the bottom

of each graph is the number of animals showing a 4-fold increase in neutralization titer at 7 days after ZIKV challenge.

## DISCUSSION

### Chapter 5: Conclusion, Perspective, and Future Directions<sup>4</sup>

Studies from other flaviviruses have suggested that the glycosylation of flavivirus protein plays a role in virion release [20], replication, virus assembly [21], neuroinvasiveness in mice [22] [23], and the deglycosylation of the viral proteins has been proposed as a live-attenuated vaccine approach [26]. The information regarding the E & NS1 proteins role in biological processes resulted from research in other flaviviruses, and we can infer it applies to ZIKV.

The glycosylation of the ZIKV E and NS1 proteins is needed to understand the mechanism of the infection cycle and host response. ZIKV has an N-linked glycosylation site in the E & NS1 proteins, highly conserved among flaviviruses [100]. The objective of this dissertation was to study the role of glycosylation in ZIKV, which was undertaken using recombinant viruses, lacking the N-glycosylation site, to characterize the glycosylation of the ZIKV E and NS1 proteins.

---

<sup>4</sup> Contents of this chapter have been previously published:

- Fontes-Garfias, C. R.; Shan, C.; Luo, H.; Muruato A.; Medeiros, D. B.A.; Mays, E.; Xie, X.; Zou, J.; Roundy, C. M.; Wakamiya, M.; Rossi, S. L.; Wang, T.; Weaver, S.C.; Shi P.-Y. Functional Analysis of Glycosylation of Zika Virus Envelope Protein. *Cell Reports* 2017; 21: 1180-1190. DOI: 10.1016/j.celrep.2017.10.016
- Fontes-Garfias, C. R.; Shi, P.-Y. Reserve genetic approaches for the development of Zika vaccines and therapeutics. *Current Opinion in Virology* 2020; 44, 7-15, doi: 10.1016/j.coviro.2020.05.002.
- Richner, J.M.\*; Jagger, B. W.\*; Shan, C.\*; Fontes, C. R.\*; Dowd, K. A.; Cao, B.; Himansu, S.; Caine, E. A.; Nunes, B. T. D.; Medeiros, D. B. A.; Muruato, A. E.; Foreman, B. M.; Luo, H.; Wang, T.; Barrett, A.D.; Weaver, S.C.; Vasconcelos, P. F. C.; Rossi, S. L.; Ciaramella, G.; Mysorekar, I. U.; Pierson, T. C.; Shi, P.-Y.; Diamond, M. S. Vaccine Mediated Protection Against Zika Virus-Induced Congenital Disease. *Cell* 2017; 170, 273-283.e12 DOI: 10.1016/j.cell.2017.06.040.

There has been a rapid emergency effort to develop a safe and effective vaccine against ZIKV to limit the epidemic force of infection and prevent its major disease manifestations, such as microcephaly and congenital malformations in the context of infection during pregnancy. Chapter 3 showed that glycosylation of the ZIKV E protein plays an important role in infecting the mosquito vector and pathogenesis in mouse. The viral E protein glycosylation is critical for ZIKV virulence in the A129 mice and it is required for infection of the *Aedes aegypti* vector. Since the E glycosylation mutation attenuated ZIKV, its potential use for live-attenuated vaccine development was explored. The viral envelope protein glycosylation is critical for the ZIKV virulence in A129 mice. The knockout of the E glycosylation significantly attenuated ZIKV in the *in vivo* model, this was evidenced by a robust neutralizing antibody response that reduced viremia and displayed no mortality following WT challenge of the A129 mice. However, the mouse neurovirulence was not reduced by the depletion of the E protein glycosylation. When newborn CD1 mice brains were injected with the E glycosylation mutant virus, the mortality rates were similar to the mice injected with the WT virus. In contrast, other vaccine candidates displayed a better safety profile than the E glycosylation mutant. For example, the NS1 glycosylation mutant did not cause any death of newborn CD1 mice.

Such *in vitro* and *in vivo* discrepancies were also observed previously when analyzing the function of E glycosylation in other flaviviruses. In the case of DENV-2, knockout of N153 glycosylation of E protein reduced viral replication in C6/36 cells [20, 35], but did not affect viral replication in intrathoracically inoculated *Ae.*

*aegypti* mosquitoes [34]. In WNV, knockout of E N154 glycosylation did not affect viral replication in C6/36 cells, but significantly reduced viral transmission in *Culex* mosquitoes [31]. These *in vitro* and *in vivo* discrepancies are likely due to the lack of cellular factor(s) and complex immune systems in cell lines. Such cellular factor(s) and immune systems could play important roles in interacting with glycosylated E protein on virion surface and in launching robust antiviral activities, respectively. In the case of ZIKV, it remains to be determined the cell types and their contributions to the neurovirulence in the infected CD1 mice. Finally, the discrepant results derived from cell culture, mouse model, and mosquito underscore the importance in performing experiments both *in vitro* and *in vivo* to confirm the findings of from different experimental flavivirus systems [24].

Recent studies have established that anti-ZIKV vaccines can protect against viremia, tissue viral burden, and/or lethal challenge in mice or non-human primate models of ZIKV infection and pathogenesis [84-89]. Several of these ZIKV vaccine platforms (DNA plasmid or modified mRNA LNPs encoding prM-E gene and chemically inactivated virions) have advanced into phase 1 human trials [90]. However, all of the pre-clinical studies have been performed in non-pregnant animals, and thus no report has established vaccine-mediated protection against placental and fetal infection and injury. Protection should be possible, as passive transfer of ZIKV-117, a highly neutralizing human anti-ZIKV antibody, limited placental infection and transmission to the fetus [56].

Chapter 4 utilized a vaccine platform based on Asian/American ZIKV strain, because it is a pre-epidemic strain without replication- and virulence-enhancing



mutations [101-104]. For the ZIKV-NS1-LAV, mutations were engineered in the NS1 gene to abolish its N-glycosylation [9]. NS1 glycosylation was previously shown to play an important role in viral replication [27] and this knowledge guided the rational design of this vaccine. After a single dose vaccination, the ZIKV-NS1-LAV showed efficacy in A129 mice with a strong antibody response (neutralizing titer of 1:7000) and no detectable viremia after challenge. The glycosylation mutant LAV was shown to protect both pregnant C57BL/6 mice and their fetuses from ZIKV infection [9]. Additionally, relative to the placebo controls, dams immunized with ZIKV-NS1-LAV showed markedly diminished levels of viral RNA in maternal, placental, and fetal tissues, and the majority of fetuses showed no evidence of transmission. Thus, at least in mice, ZIKV vaccines administered before pregnancy can prevent placental and fetal infection. The ZIKV-NS1-LAV virus was also not infectious in mosquitoes. Surprisingly, non-human primates (NHPs) vaccinated with ZIKV-NS1-LAV did not develop protective, neutralizing titers. It is not currently known what factors contribute to the discrepancy between the mouse and NHP studies.

Since 2016, ZIKV vaccine remains a global health priority as shown by the continued progress in ZIKV vaccine development. However, an approved vaccine or antiviral is still not available to prevent and/or treat ZIKV infection. Therefore, it will be interesting to continue to explore the glycosylation mutants identified to enhance the development of live-attenuated vaccine.

LAVs are designed to mimic the natural viral infection and, as such, often require only a single dose immunization and induce rapid and durable immunity,

which is of practical importance since ZIKV was endemic in developing countries [48]. The optimal vaccine will need to prevent infection in reproductive tissues and establish protection in the context of pregnancy [105]. In addition to the regular vaccine safety requirements, due to the infectious nature of LAV, these candidates should bear no risk of transmission via mosquitoes [106].

Together the results reported in Chapters 3 & 4 indicate that ZIKV with the E or NS1 mutations or alone are not a safe vaccine candidate. However, the E and NS1 glycosylation mutations could be combined with other attenuation approaches for live-attenuated vaccine development. For examples, the NS4B-P38 is highly conserved among mosquito-borne flaviviruses, including West Nile virus (WNV). For example, the WNV NS4B-P38G mutant had significantly reduced neuroinvasiveness [107], but triggered stronger protective immune responses in mice than did the parent strain WT WNV NY99 [108]. The mutation at the ZIKV NS4B-P36 (equivalent to WNV NS4B-P38) also led to modestly attenuated neuroinvasiveness in mice deficient in IFN- $\alpha/\beta$  and IFN- $\gamma$  receptors (AG129) [49]. However, NS4B mutations in WNV resulted in increased competence compared to WT viruses in mosquitoes [109]. The safety profile of our E glycosylation mutant was not as optimal as other LAV candidates due to the displayed decreased neurovirulence in mice. To increase the genetic stability with concurrent greater attenuation and reduced infectivity in *Aedes* mosquitoes both mutations, NS4B-P36A and E-N154Q, could be combined to develop an attractive LAV candidate.

N-glycosylation is a commonly observed protein modification fundamental to the structure, function, and stability of proteins. Attachment of an N-glycan to

the primary structure of a protein is a co-translational restricted to the consensus motif N-X-S/T, where asparagine is located N-terminal to any amino acid (except proline) followed by either serine or threonine [110]. Another approach to minimize the reversion of glycosylation is to abrogate the glycosylation site by introducing a mutation at both the asparagine and serine/threonine sites.

Deglycosylation of the E and NS1 protein as a potential candidate has been reported in WNV. Whiteman *et al.* showed that the deglycosylation of both proteins completely attenuates for neuroinvasiveness and induces protective immunity in mice [28]. However, the approach of combining mutations that abolish both glycosylation sites have not been studied in ZIKV. It would be interesting to see if the reduced neurovirulence observed in the ZIKV NS1 glycosylation mutant continues when combined with the E mutant. Additionally, the NS1 glycosylation mutant displayed promising results in mouse models but failed to do the same in the NHP model. Flavivirus enters host cells via receptor-mediated endocytosis, the initial attachment is through C-type lectins. It is possible that the attachment might be dependent on the expression level of lectins on mammalian surface. This might explain the discrepancy found in vitro and in vivo, and among mouse and NHP models.

Oncolytic viruses are emerging as promising cancer therapeutic options [111]. Glioblastoma (GBM) is the most common and malignant form of primary brain tumor and despite aggressive treatment with surgery, radiation, and chemotherapy, GBM remains the most lethal of all human cancers [112, 113]. Thus, novel treatment options are urgently needed. ZIKV's ability to cause

microcephaly by killing neural progenitor cells (NPCs) in the fetus raised the possibility of its utility as an oncolytic virus to target glioblastoma stem cells (GSCs) [114]. GSCs have self-renewal, tumorigenic and differentiation potential, and thus are similar to NPCs. *Zhu, et al.* first demonstrated that ZIKV selectively kills human GSCs in vitro [112]. This was followed by *Chen et al.* testing ZIKV-3'UTR-Δ10's oncolytic activity against human GSCs [113]. These results showed that ZIKV-3'UTR-Δ10, a safer strain than WT ZIKV, retained the oncolytic activity against patient-derived GSCs in vivo despite being significantly attenuated when compared to WT ZIKV, paving the way for clinical development of this vaccine candidate for GBM therapy [113]. Due to safety being paramount in any potential clinical application. To further develop ZIKV as an oncolytic therapy, a safer strain could be generated by combining the ZIKV-3'UTR-Δ10 [115] with the N-N154Q or NS1-N130Q+N207Q.

Due to the lack of antiviral drugs to treat flavivirus diseases, vaccines are proposed as an efficient alternative to control diseases. Vaccine development should take into consideration not only the efficacy and safety profile but the distribution channels. Standard DNA vaccines have the advantage of chemical stability, simple manufacturing, no cold chain requirement, and low cost. These candidates typically consist of a plasmid encoding one or more viral protein(s) under control of a constitutive, eukaryotic promoter. However, DNA vaccines (expressing single or multiple antigens) usually require multiple doses and/or periodic boosting [10]. Since ZIKV is endemic in developing countries, immunizing populations in remote areas with multiple doses renders the DNA vaccination

approach less practical and more challenging. In contrast, as described in (I), LAVs, which lack the shipping and shelf stability of DNA vaccines, have the advantage of a single dose eliciting rapid, durable protection. Zou, *et al.* developed a DNA-launched LAV that combines the strengths of both LAV and DNA vaccine platforms by engineering a eukaryotic promoter upstream of the full-length cDNA copy of an attenuated ZIKV encoded on a plasmid. Therefore, it would be interesting to develop the E and/or NS1 glycosylation mutant approach in this platform.

This dissertation project targeted glycosylation of ZIKV proteins as an approach for developing vaccines and understanding the function it has in viral replication. Site-directed mutagenesis was performed to generate non-glycosylated ZIKV to determine how the lack of glycosylation affects viral infectivity by analyzing: virus plaque size, cytopathic effect, plaque morphology, growth kinetics in mammalian and mosquito cells, thermostability and thermosensitivity. In addition, the virulence of ZIKV mutants was compared to the ZIKV WT in mouse models and determined mosquito infection and dissemination using *Ae. aegypti*. The results shown in Chapter 3 and 4 provided experimental evidence, *in vivo* and *in vitro*, that glycosylation affects in the ZIKV infection cycle, pathogenesis, and vaccine development

## References

1. Weaver, S.C., et al., *Zika virus: History, emergence, biology, and prospects for control*. Antiviral Res, 2016. **130**: p. 69-80.
2. Coyne, C.B. and H.M. Lazear, *Zika virus - reigniting the TORCH*. Nat Rev Microbiol, 2016. **14**(11): p. 707-715.
3. Petersen, L.R., et al., *Zika Virus*. N Engl J Med, 2016. **374**(16): p. 1552-63.
4. Lazear, H.M., E.M. Stringer, and A.M. de Silva, *The Emerging Zika Virus Epidemic in the Americas: Research Priorities*. JAMA, 2016. **315**(18): p. 1945-6.
5. Ikejezie, J., et al., *Zika Virus Transmission - Region of the Americas, May 15, 2015-December 15, 2016*. MMWR Morb Mortal Wkly Rep, 2017. **66**(12): p. 329-334.
6. Shi, P.-Y., *Molecular virology and control of flaviviruses*. 2012, Norfolk, UK: Caister Academic Press. vii, 358 p.
7. Aliota, M.T., et al., *Zika in the Americas, year 2: What have we learned? What gaps remain? A report from the Global Virus Network*. Antiviral Res, 2017. **144**: p. 223-246.
8. Fauci, A.S. and D.M. Morens, *Zika Virus in the Americas--Yet Another Arbovirus Threat*. N Engl J Med, 2016. **374**(7): p. 601-4.
9. Richner, J.M., et al., *Vaccine Mediated Protection Against Zika Virus-Induced Congenital Disease*. Cell, 2017. **170**(2): p. 273-283.e12.

10. Shan, C., X. Xie, and P.Y. Shi, *Zika Virus Vaccine: Progress and Challenges*. Cell Host Microbe, 2018. **24**(1): p. 12-17.
11. Xie, X., et al., *Zika Virus Replicons for Drug Discovery*. EBioMedicine, 2016. **12**: p. 156-160.
12. Shan, C., et al., *An Infectious cDNA Clone of Zika Virus to Study Viral Virulence, Mosquito Transmission, and Antiviral Inhibitors*. Cell Host Microbe, 2016. **19**(6): p. 891-900.
13. Pierson, T.C. and B.S. Graham, *Zika Virus: Immunity and Vaccine Development*. Cell, 2016. **167**(3): p. 625-631.
14. Pierson, T. and M.S. Diamond, *Flavivirus*, in *Fields of Virology*. 2013, Wolters Kluwer Health Adis (ESP).
15. Hamel, R., et al., *Biology of Zika Virus Infection in Human Skin Cells*. J Virol, 2015. **89**(17): p. 8880-96.
16. Li, G., et al., *Characterization of cytopathic factors through genome-wide analysis of the Zika viral proteins in fission yeast*. Proc Natl Acad Sci U S A, 2017. **114**(3): p. E376-E385.
17. Xie, X., et al., *Understanding Zika Virus Stability and Developing a Chimeric Vaccine through Functional Analysis*. MBio, 2017. **8**(1).
18. Alberts, B., *Molecular biology of the cell*. 5th ed. 2008, New York: Garland Science.
19. Vigerust, D.J. and V.L. Shepherd, *Virus glycosylation: role in virulence and immune interactions*. Trends Microbiol, 2007. **15**(5): p. 211-8.

20. Lee, E., et al., *Both E protein glycans adversely affect dengue virus infectivity but are beneficial for virion release*. J Virol, 2010. **84**(10): p. 5171-80.
21. Li, J., et al., *The glycosylation site in the envelope protein of West Nile virus (Sarafend) plays an important role in replication and maturation processes*. J Gen Virol, 2006. **87**(Pt 3): p. 613-22.
22. Shirato, K., et al., *Viral envelope protein glycosylation is a molecular determinant of the neuroinvasiveness of the New York strain of West Nile virus*. J Gen Virol, 2004. **85**(Pt 12): p. 3637-45.
23. Beasley, D.W., et al., *Envelope protein glycosylation status influences mouse neuroinvasion phenotype of genetic lineage 1 West Nile virus strains*. J Virol, 2005. **79**(13): p. 8339-47.
24. Fontes-Garfias, C.R., et al., *Functional Analysis of Glycosylation of Zika Virus Envelope Protein*. Cell Rep, 2017. **21**(5): p. 1180-1190.
25. Annamalai, A.S., et al., *Zika Virus Encoding Non-Glycosylated Envelope Protein is Attenuated and Defective in Neuroinvasion*. J Virol, 2017.
26. Whiteman, M.C., et al., *Development and characterization of non-glycosylated E and NS1 mutant viruses as a potential candidate vaccine for West Nile virus*. Vaccine, 2010. **28**(4): p. 1075-83.
27. Muylaert, I.R., et al., *Mutagenesis of the N-linked glycosylation sites of the yellow fever virus NS1 protein: effects on virus replication and mouse neurovirulence*. Virology, 1996. **222**(1): p. 159-68.



28. Whiteman, M.C., et al., *Development and characterization of non-glycosylated E and NS1 mutant viruses as a potential candidate vaccine for West Nile virus*. Vaccine, 2010. **28**(4): p. 1075-1083.
29. Hanna, S.L., et al., *N-linked glycosylation of west nile virus envelope proteins influences particle assembly and infectivity*. J Virol, 2005. **79**(21): p. 13262-74.
30. Scherret, J.H., et al., *Biological significance of glycosylation of the envelope protein of Kunjin virus*. Ann N Y Acad Sci, 2001. **951**: p. 361-3.
31. Moudy, R.M., et al., *West Nile virus envelope protein glycosylation is required for efficient viral transmission by Culex vectors*. Virology, 2009. **387**(1): p. 222-8.
32. Saxena, V., et al., *A hamster-derived West Nile virus isolate induces persistent renal infection in mice*. PLoS Negl Trop Dis, 2013. **7**(6): p. e2275.
33. Davis, C.W., et al., *West Nile virus discriminates between DC-SIGN and DC-SIGNR for cellular attachment and infection*. J Virol, 2006. **80**(3): p. 1290-301.
34. Bryant, J.E., et al., *Glycosylation of the dengue 2 virus E protein at N67 is critical for virus growth in vitro but not for growth in intrathoracically inoculated Aedes aegypti mosquitoes*. Virology, 2007. **366**(2): p. 415-23.
35. Mondotte, J.A., et al., *Essential role of dengue virus envelope protein N glycosylation at asparagine-67 during viral propagation*. J Virol, 2007. **81**(13): p. 7136-48.

36. Lozach, P.Y., et al., *Dendritic cell-specific intercellular adhesion molecule 3-grabbing non-integrin (DC-SIGN)-mediated enhancement of dengue virus infection is independent of DC-SIGN internalization signals*. J Biol Chem, 2005. **280**(25): p. 23698-708.
37. Perera-Lecoin, M., et al., *Flavivirus entry receptors: an update*. Viruses, 2013. **6**(1): p. 69-88.
38. Hacker, K., L. White, and A.M. de Silva, *N-linked glycans on dengue viruses grown in mammalian and insect cells*. J Gen Virol, 2009. **90**(Pt 9): p. 2097-106.
39. Tassaneetrithep, B., et al., *DC-SIGN (CD209) mediates dengue virus infection of human dendritic cells*. J Exp Med, 2003. **197**(7): p. 823-9.
40. Pokidysheva, E., et al., *Cryo-EM reconstruction of dengue virus in complex with the carbohydrate recognition domain of DC-SIGN*. Cell, 2006. **124**(3): p. 485-93.
41. Cheng, G., et al., *A C-type lectin collaborates with a CD45 phosphatase homolog to facilitate West Nile virus infection of mosquitoes*. Cell, 2010. **142**(5): p. 714-25.
42. Liu, Y., et al., *Transmission-blocking antibodies against mosquito C-type lectins for dengue prevention*. PLoS Pathog, 2014. **10**(2): p. e1003931.
43. Dick, G.W., S.F. Kitchen, and A.J. Haddow, *Zika virus. I. Isolations and serological specificity*. Trans R Soc Trop Med Hyg, 1952. **46**(5): p. 509-20.
44. Tebas, P., et al., *Safety and Immunogenicity of an Anti-Zika Virus DNA Vaccine - Preliminary Report*. N Engl J Med, 2017.

45. Gaudinski, M.R., et al., *Safety, tolerability, and immunogenicity of two Zika virus DNA vaccine candidates in healthy adults: randomised, open-label, phase 1 clinical trials*. Lancet, 2018. **391**(10120): p. 552-562.
46. Modjarrad, K., et al., *Preliminary aggregate safety and immunogenicity results from three trials of a purified inactivated Zika virus vaccine candidate: phase 1, randomised, double-blind, placebo-controlled clinical trials*. Lancet, 2018. **391**(10120): p. 563-571.
47. Organization, W.H. *WHO vaccine pipeline tracker*. March 2020]; Available from:  
  
[https://www.who.int/immunization/research/vaccine\\_pipeline\\_tracker\\_spreadsheet/en/](https://www.who.int/immunization/research/vaccine_pipeline_tracker_spreadsheet/en/).
48. Xie, X., et al., *A Single-Dose Live-Attenuated Zika Virus Vaccine with Controlled Infection Rounds that Protects against Vertical Transmission*. Cell Host Microbe, 2018. **24**(4): p. 487-499.e5.
49. Li, G., et al., *An attenuated Zika virus NS4B protein mutant is a potent inducer of antiviral immune responses*. NPJ Vaccines, 2019. **4**: p. 48.
50. Zou, J., et al., *A single-dose plasmid-launched live-attenuated Zika vaccine induces protective immunity*. EBioMedicine, 2018. **36**: p. 92-102.
51. Garg, H., et al., *Development of Virus-Like-Particle Vaccine and Reporter Assay for Zika Virus*. J Virol, 2017. **91**(20).
52. Xie, X. and P.Y. Shi, *Repurposing an HIV Drug for Zika Virus Therapy*. Mol Ther, 2019. **27**(12): p. 2064-2066.

53. Somnuk, P., et al., *N-linked glycosylation of dengue virus NS1 protein modulates secretion, cell-surface expression, hexamer stability, and interactions with human complement*. Virology, 2011. **413**(2): p. 253-64.
54. Yang, Y., et al., *A cDNA Clone-Launched Platform for High-Yield Production of Inactivated Zika Vaccine*. EBioMedicine, 2017. **17**: p. 145-156.
55. Zhao, H., et al., *Structural Basis of Zika Virus-Specific Antibody Protection*. Cell, 2016. **166**(4): p. 1016-27.
56. Sapparapu, G., et al., *Neutralizing human antibodies prevent Zika virus replication and fetal disease in mice*. Nature, 2016. **540**(7633): p. 443-447.
57. Lazear, H.M., et al., *A Mouse Model of Zika Virus Pathogenesis*. Cell Host Microbe, 2016. **19**(5): p. 720-730.
58. Brien, J.D., H.M. Lazear, and M.S. Diamond, *Propagation, quantification, detection, and storage of West Nile virus*. Curr Protoc Microbiol, 2013. **31**: p. 15D 3 1-15D 3 18.
59. Rossi, S.L., et al., *Characterization of a Novel Murine Model to Study Zika Virus*. Am J Trop Med Hyg, 2016. **94**(6): p. 1362-9.
60. Miner, J.J., et al., *Zika Virus Infection during Pregnancy in Mice Causes Placental Damage and Fetal Demise*. Cell, 2016. **165**(5): p. 1081-91.
61. Daffis, S., et al., *Interferon regulatory factor IRF-7 induces the antiviral alpha interferon response and protects against lethal West Nile virus infection*. J Virol, 2008. **82**(17): p. 8465-75.

62. Wang, T., et al., *Toll-like receptor 3 mediates West Nile virus entry into the brain causing lethal encephalitis*. Nat. Med., 2004. **10**(12): p. 1366-73.
63. Fauci, A.S. and D.M. Morens, *Zika Virus in the Americas - Yet Another Arbovirus Threat*. N Engl J Med, 2016.
64. Costello, A., et al., *Defining the syndrome associated with congenital Zika virus infection*. Bull World Health Organ, 2016. **94**(6): p. 406-406A.
65. Shan, C., et al., *Zika Virus: Diagnosis, Therapeutics, and Vaccine ACS Infectious Diseases*, 2016. **2**: p. 170-2.
66. Pierson, T.C. and M.S. Diamond, Flaviviruses p. 747-794. In D.M. Knipe and P.M. Howley (ed), Fields virology, 6th., vol. 1.
67. Hamel, R., et al., *Biology of Zika Virus Infection in Human Skin Cells*. J Virol, 2015. **89**(17): p. 8880-96.
68. Rey, F.A., K. Stiasny, and F.X. Heinz, *Flavivirus structural heterogeneity: implications for cell entry*. Curr Opin Virol, 2017. **24**: p. 132-139.
69. Welsch, S., et al., *Composition and three-dimensional architecture of the dengue virus replication and assembly sites*. Cell Host Microbe, 2009. **5**(4): p. 365-75.
70. Acosta, E.G., A. Kumar, and R. Bartenschlager, *Revisiting dengue virus-host cell interaction: new insights into molecular and cellular virology*. Adv Virus Res, 2014. **88**: p. 1-109.
71. Adams, S.C., et al., *Glycosylation and antigenic variation among Kunjin virus isolates*. Virology, 1995. **206**(1): p. 49-56.

72. Beasley, D.W., et al., *Genome sequence and attenuating mutations in West Nile virus isolate from Mexico*. Emerg Infect Dis, 2004. **10**(12): p. 2221-4.
73. Berthet, F.X., et al., *Extensive nucleotide changes and deletions within the envelope glycoprotein gene of Euro-African West Nile viruses*. J Gen Virol, 1997. **78 ( Pt 9)**: p. 2293-7.
74. Vorndam, V., et al., *Molecular and biological characterization of a non-glycosylated isolate of St Louis encephalitis virus*. J Gen Virol, 1993. **74 ( Pt 12)**: p. 2653-60.
75. Post, P.R., et al., *Heterogeneity in envelope protein sequence and N-linked glycosylation among yellow fever virus vaccine strains*. Virology, 1992. **188**(1): p. 160-7.
76. Shirato, K., et al., *Viral envelope protein glycosylation is a molecular determinant of the neuroinvasiveness of the New York strain of West Nile virus*. Journal of General Virology, 2004. **85**(Pt 12): p. 3637-45.
77. Murata, R., et al., *Glycosylation of the West Nile Virus envelope protein increases in vivo and in vitro viral multiplication in birds*. Am J Trop Med Hyg, 2010. **82**(4): p. 696-704.
78. Sirohi, D., et al., *The 3.8 Å resolution cryo-EM structure of Zika virus*. Science, 2016. **352**(6284): p. 467-70.
79. Shan, C., et al., *A live-attenuated Zika virus vaccine candidate induces sterilizing immunity in mouse models*. Nat Med, 2017.

80. Roundy, C.M., et al., *Variation in Aedes aegypti Mosquito Competence for Zika Virus Transmission*. Emerg Infect Dis, 2017. **23**(4): p. 625-632.
81. Bernhard, O.K., et al., *Proteomic analysis of DC-SIGN on dendritic cells detects tetramers required for ligand binding but no association with CD4*. J Biol Chem, 2004. **279**(50): p. 51828-35.
82. Lozach, P.Y., et al., *Dendritic cell-specific intercellular adhesion molecule 3-grabbing non-integrin (DC-SIGN)-mediated enhancement of dengue virus infection is independent of DC-SIGN internalization signals*. J Biol Chem, 2005. **280**(25): p. 23698-708.
83. Richner, J., et al., *Vaccine mediated protection against Zika virus induced congenital disease*. Cell, 2017. **170**: p. 273–283.
84. Larocca, R.A., et al., *Vaccine protection against Zika virus from Brazil*. Nature, 2016. **536**(7617): p. 474-478.
85. Abbink, P., et al., *Protective efficacy of multiple vaccine platforms against Zika virus challenge in rhesus monkeys*. Science, 2016. **353**(6304): p. 1129-32.
86. Dowd, K.A., et al., *Rapid development of a DNA vaccine for Zika virus*. Science, 2016. **354**(6309): p. 237-240.
87. Muthumani, K., et al., *In vivo protection against ZIKV infection and pathogenesis through passive antibody transfer and active immunisation with a prMEnv DNA vaccine*. npj Vaccines, 2016: p. doi:10.1038/npjvaccines.2016.21.

88. Richner, J.M., et al., *Modified mRNA Vaccines Protect against Zika Virus Infection*. Cell, 2017. **168**(6): p. 1114-1125.e10.
89. Pardi, N. and D. Weissman, *Nucleoside Modified mRNA Vaccines for Infectious Diseases*. Methods Mol Biol, 2017. **1499**: p. 109-121.
90. Durbin, A.P., *Vaccine Development for Zika Virus-Timelines and Strategies*. Semin Reprod Med, 2016. **34**(5): p. 299-304.
91. Pryor, M.J., et al., *Growth restriction of dengue virus type 2 by site-specific mutagenesis of virus-encoded glycoproteins*. J Gen Virol, 1998. **79**(Pt 11): p. 2631-9.
92. Whiteman, M.C., et al., *Multiple amino acid changes at the first glycosylation motif in NS1 protein of West Nile virus are necessary for complete attenuation for mouse neuroinvasiveness*. Vaccine, 2011. **29**(52): p. 9702-10.
93. Muller, D.A. and P.R. Young, *The flavivirus NS1 protein: molecular and structural biology, immunology, role in pathogenesis and application as a diagnostic biomarker*. Antiviral Res, 2013. **98**(2): p. 192-208.
94. Uraki, R., et al., *Zika virus causes testicular atrophy*. Sci Adv, 2017. **3**(2): p. e1602899.
95. Govero, J., et al., *Zika virus infection damages the testes in mice*. Nature, 2016. **540**: p. 438-442.
96. Ma, W., et al., *Zika Virus Causes Testis Damage and Leads to Male Infertility in Mice*. Cell, 2016. **167**: p. 1511-1524.



97. Yockey, L.J., et al., *Vaginal Exposure to Zika Virus during Pregnancy Leads to Fetal Brain Infection*. Cell, 2016. **166**(5): p. 1247-1256.e4.
98. Khan, S., et al., *Dampened antiviral immunity to intravaginal exposure to RNA viral pathogens allows enhanced viral replication*. J Exp Med, 2016. **213**(13): p. 2913-2929.
99. Shin, H. and A. Iwasaki, *Generating protective immunity against genital herpes*. Trends Immunol, 2013. **34**(10): p. 487-94.
100. Kostyuchenko, V.A., et al., *Structure of the thermally stable Zika virus*. Nature, 2016. **533**(7603): p. 425-8.
101. Liu, Y., et al., *Evolutionary enhancement of Zika virus infectivity in Aedes aegypti mosquitoes*. Nature, 2017. **545**(7655): p. 482-486.
102. Xia, H., et al., *An evolutionary NS1 mutation enhances Zika virus evasion of host interferon induction*. Nat Commun, 2018. **9**(1): p. 414.
103. Yuan, L., et al., *A single mutation in the prM protein of Zika virus contributes to fetal microcephaly*. Science, 2017. **358**(6365): p. 933-936.
104. Zhang, X., et al., *Zika Virus NS2A-Mediated Virion Assembly*. mBio, 2019. **10**(5).
105. Barrett, A.D.T., *Current status of Zika vaccine development: Zika vaccines advance into clinical evaluation*. NPJ Vaccines, 2018. **3**: p. 24.
106. Muruato, A.E., et al., *Genetic stability of live-attenuated Zika vaccine candidates*. Antiviral Res, 2019. **171**: p. 104596.
107. Wicker, J.A., et al., *Mutational analysis of the West Nile virus NS4B protein*. Virology, 2012. **426**(1): p. 22-33.

108. Welte, T., et al., *Immune responses to an attenuated West Nile virus NS4B-P38G mutant strain*. Vaccine, 2011. **29**(29-30): p. 4853-61.
109. Van Slyke, G.A., et al., *Vertebrate attenuated West Nile virus mutants have differing effects on vector competence in Culex tarsalis mosquitoes*. J Gen Virol, 2013. **94**(Pt 5): p. 1069-1072.
110. Lowenthal, M.S., et al., *Identification of Novel N-Glycosylation Sites at Noncanonical Protein Consensus Motifs*. J Proteome Res, 2016. **15**(7): p. 2087-101.
111. Chiocca, E.A. and S.D. Rabkin, *Oncolytic viruses and their application to cancer immunotherapy*. Cancer Immunol Res, 2014. **2**(4): p. 295-300.
112. Zhu, Z., et al., *Zika virus has oncolytic activity against glioblastoma stem cells*. J Exp Med, 2017. **214**(10): p. 2843-2857.
113. Chen, Q., et al., *Treatment of Human Glioblastoma with a Live Attenuated Zika Virus Vaccine Candidate*. mBio, 2018. **9**(5).
114. Tang, H., et al., *Zika Virus Infects Human Cortical Neural Progenitors and Attenuates Their Growth*. Cell Stem Cell, 2016. **18**(5): p. 587-90.
115. Shan, C., et al., *Maternal vaccination and protective immunity against Zika virus vertical transmission*. Nat Commun, 2019. **10**(1): p. 5677.

## **Vita**

Camila R. Fontes-Garfias was born November 4<sup>th</sup> to Vicky and Rafael Fontes. After graduating from high school, she honorably served in the U.S. Army for nine years. In 2010 while on active duty, Camila received a B.A. in Natural Science and Mathematics from Thomas Edison State College. After completion of her military service Camila decided to better prepare for Graduate school by pursuing another degree, and in May 2015 she graduated from Houston Baptist University with B.S. in Biochemistry and Molecular Biology. In the Fall of 2015, she joined the biochemistry and molecular biology graduate program at The University of Texas Medical Branch. After joining the Shi lab, Camila's research on Zika virus has led to vaccine candidates that efficiently protect viral infection and fetal microcephaly. Her work has been published in *Cell*, *Cell Reports*, and other premier journals in the field of biomedical sciences. In response the current COVID-19 crisis, Camila has stepped up to develop novel technology that is essential for patients serodiagnosis, vaccine, and antiviral drug development. The assay is being utilized for field study and countermeasure development to combat COVID-19 pandemic.

Permanent address:        7019 Lasker Drive Apt 915  
   Galveston, TX 77551

This dissertation was typed by Camila R. Fontes-Garfias.

## **Education**

Ph.D. Biochemistry and Molecular Biology 2015-present (expected graduation December 2020)

University of Texas Medical Branch  
Galveston, TX

B.S. Biochemistry and Molecular Biology 2012-2015

Houston Baptist University  
Houston, TX

B.A. Natural Science 2008-2010

Thomas Edison State College  
Trenton, NJ

### **Positions**

Ph.D. candidate, 2016-present

Department of Biochemistry and Molecular Biology,  
University of Texas Medical Branch, TX 77550, USA

1. Characterization of the ZIKV E and NS1 protein glycosylation
2. Characterization of the ZIKV virus structural genes between the African and Asian strains
3. Development of a reporter SARS-CoV-2 assay that can be standardized to support broad serodiagnosis and vaccine evaluation

Military Service 2002-2011

Active Duty U.S. Army

1. US Army recruiter
2. Automated Logistical Sergeant

### **Publications**

1. Sahin, U., A. Muik, E. Derhovanessian, I. Vogler, L. M. Kranz, M. Vormehr, A. Baum, K. Pascal, J. Quandt, D. Maurus, S. Brachtendorf, V. Lörks, J. Sikorski, R. Hilker, D. Becker, A. K. Eller, J. Grützner, C. Boesler, C. Rosenbaum, M. C. Kühnle, U. Luxemburger, A. Kemmer-Brück, D. Langer, M. Bexon, S. Bolte, K. Karikó, T. Palanche, B. Fischer, A. Schultz, P. Y. Shi, **C. Fontes-Garfias**, J. L. Perez, K. A. Swanson, J. Loschko, I. L. Scully, M. Cutler, W. Kalina, C. A. Kyratsous, D. Cooper, P. R. Dormitzer, K. U. Jansen and Ö. Türeci (2020). "COVID-19 vaccine BNT162b1 elicits human antibody and T." **Nature** 586(7830): 594-599.
2. Xie, X., M. C. Nielsen, A. E. Muruato, **C. R. Fontes-Garfias** and P. Ren (2020). "Evaluation of a SARS-CoV-2 lateral flow assay using the plaque reduction neutralization test." **Diagn Microbiol Infect Dis** 99(2): 115248.
3. Muruato\*, A. E., **C. R. Fontes-Garfias**\*, P. Ren, M. A. Garcia-Blanco, V. D. Menachery, X. Xie and P. Y. Shi (2020). "A high-throughput neutralizing antibody assay for COVID-19 diagnosis and vaccine evaluation." **Nat Commun** 11(1): 4059. (\*co-first author)

4. Xie, X., A. E. Muruato, X. Zhang, K. G. Lokugamage, **C. R. Fontes-Garfias**, J. Zou, J. Liu, P. Ren, M. Balakrishnan, T. Cihlar, C. K. Tseng, S. Makino, V. D. Menachery, J. P. Bilello and P. Y. Shi (2020). "A nanoluciferase SARS-CoV-2 for rapid neutralization testing and screening of anti-infective drugs for COVID-19." **Nat Commun** 11(1): 5214.
5. Mulligan, M. J., K. E. Lyke, N. Kitchin, J. Absalon, A. Gurtman, S. Lockhart, K. Neuzil, V. Raabe, R. Bailey, K. A. Swanson, P. Li, K. Koury, W. Kalina, D. Cooper, **C. Fontes-Garfias**, P. Y. Shi, Ö. Türeci, K. R. Tompkins, E. E. Walsh, R. Frenck, A. R. Falsey, P. R. Dormitzer, W. C. Gruber, U. Şahin and K. U. Jansen (2020). "Phase I/II study of COVID-19 RNA vaccine BNT162b1 in adults." **Nature** 586(7830): 589-593.
6. **Fontes-Garfias, C. R.**, C. K. Baker and P. Y. Shi (2020). "Reverse genetic approaches for the development of Zika vaccines and therapeutics." **Curr Opin Virol** 44: 7-15.
7. Walsh, E. E., R. W. Frenck, A. R. Falsey, N. Kitchin, J. Absalon, A. Gurtman, S. Lockhart, K. Neuzil, M. J. Mulligan, R. Bailey, K. A. Swanson, P. Li, K. Koury, W. Kalina, D. Cooper, **C. Fontes-Garfias**, P. Y. Shi, Ö. Türeci, K. R. Tompkins, K. E. Lyke, V. Raabe, P. R. Dormitzer, K. U. Jansen, U. Şahin and W. C. Gruber (2020). "Safety and Immunogenicity of Two RNA-Based Covid-19 Vaccine Candidates." **N Engl J Med**.
8. Plante, J. A., Y. Liu, J. Liu, H. Xia, B. A. Johnson, K. G. Lokugamage, X. Zhang, A. E. Muruato, J. Zou, **C. R. Fontes-Garfias**, D. Mirchandani, D. Scharon, J. P. Bilello, Z. Ku, Z. An, B. Kalveram, A. N. Freiberg, V. D. Menachery, X. Xie, K. S. Plante, S. C. Weaver and P. Y. Shi (2020). "Spike mutation D614G alters SARS-CoV-2 fitness." **Nature**.
9. Nunes, B. T. D., **C. R. Fontes-Garfias**, C. Shan, A. E. Muruato, J. G. C. Nunes, R. M. R. Burbano, P. F. C. Vasconcelos, P. Y. Shi and D. B. A. Medeiros (2020). "Zika structural genes determine the virulence of African and Asian lineages." **Emerg Microbes Infect**: 1-27.
10. Shan, C., H. Xia, S. L. Haller, S. R. Azar, Y. Liu, J. Liu, A. E. Muruato, R. Chen, S. L. Rossi, M. Wakamiya, N. Vasilakis, R. Pei, **C. R. Fontes-Garfias**, S. K. Singh, X. Xie, S. C. Weaver and P. Y. Shi (2020). "A Zika virus envelope mutation preceding the 2015 epidemic enhances virulence and fitness for transmission." **Proc Natl Acad Sci U S A** 117(33): 20190-20197.
11. Nava, J. A. R., Y.-T. Wang, **C. R. Fontes-Garfias**, T. Syed, A. Gonzalez, K. Viramontes, K. M. Valentine, A. V. Terskikh, J. G. Gleeson, P.-Y. Shi and S. Shrestha (2020). "Zika virus evolution in the presence of dengue virus-elicited cross-reactive immunity." **The Journal of Immunology** 204(1 Supplement): 249.247-249.247.
12. Li, G., A. Adam, H. Luo, C. Shan, Z. Cao, **C. R. Fontes-Garfias**, V. V. Sarathy, C. Teleki, E. R. Winkelmann, Y. Liang, J. Sun, N. Bourne, A. D. T. Barrett, P. Y. Shi and T. Wang (2019). "An attenuated Zika virus NS4B protein mutant is a potent inducer of antiviral immune responses." **NPJ Vaccines** 4: 48.

13. Muruato, A. E., C. Shan, **C. R. Fontes-Garfias**, Y. Liu, Z. Cao, Q. Gao, S. C. Weaver and P. Y. Shi (2019). "Genetic stability of live-attenuated Zika vaccine candidates." **Antiviral Res** 171: 104596.
14. Park, H. J., P. Ji, S. Kim, Z. Xia, B. Rodriguez, L. Li, J. Su, K. Chen, C. P. Masamha, D. Baillat, **C. R. Fontes-Garfias**, A. B. Shyu, J. R. Neilson, E. J. Wagner and W. Li (2018). "3' UTR shortening represses tumor-suppressor genes in trans by disrupting ceRNA crosstalk." **Nat Genet.**
15. **Fontes-Garfias, C. R.**, C. Shan, H. Luo, A. E. Muruato, D. B. A. Medeiros, E. Mays, X. Xie, J. Zou, C. M. Roundy, M. Wakamiya, S. L. Rossi, T. Wang, S. C. Weaver and P. Y. Shi (2017). "Functional Analysis of Glycosylation of Zika Virus Envelope Protein." **Cell Rep** 21(5): 1180-1190.
16. Richner\*, J. M., B. W. Jagger\*, C. Shan\*, **C. R. Fontes\***, K. A. Dowd\*, B. Cao, S. Himansu, E. A. Caine, B. T. D. Nunes, D. B. A. Medeiros, A. E. Muruato, B. M. Foreman, H. Luo, T. Wang, A. D. Barrett, S. C. Weaver, P. F. C. Vasconcelos, S. L. Rossi, G. Ciaramella, I. U. Mysorekar, T. C. Pierson, P. Y. Shi and M. S. Diamond (2017). "Vaccine Mediated Protection Against Zika Virus-Induced Congenital Disease." **Cell** 170(2): 273-283.e212. (\*co-first author)
17. Awadalkareem Adam, **Camila R. Fontes-Garfias**, Vanessa V. Sarathy, Yang Liu, Huanle Luo, Wenqian Li, Antonio E. Muruato, Binbin Wang, Renat Ahatov, Yoseph Mahmoud, Chao Shan, Samantha Osman, Alfredo Torres, Alan DT Barrett, Pei-Yong Shi, and Tian Wang. "Characterization of a Zika Virus Envelope Glycosylation and Non-structure 4B P36 Double Mutant." Under Review
18. **Camila R. Fontes-Garfias**, Yang Liu, Chao Shan, Antonio E. Muruato, Pei-Yong Shi. "Zika virus prM mutation enhances neurovirulence and neuroinvasiveness of African and Asian lineages." Manuscript in preparation.
19. Sharmila Nair\*, Luciano Mazzocchi\*, Arijita Jash\*, Jennifer Govero, Sachendra S. Bais, Tong Hu, **Camila R. Fontes-Garfias**, Chao Shan, Hideho Okada, Sujana Shrestha, Jeremy N. Rich, Pei Yong Shi, Michael S. Diamond, and Milan G. Chheda<sup>1</sup>. "Zika virus oncolytic activity requires CD8<sup>+</sup> T cells and is boosted by immune checkpoint blockade." JCI Insight, accepted.